



 Cite this: *RSC Adv.*, 2025, 15, 18920

From lab to field: revolutionizing antibiotic detection with aptamer-based biosensors†

 Dipanjan Das, Joydeep Chakraborty, Pankaj Mandal, Rittick Mondal * and Amit Kumar Mandal *

 Received 25th March 2025
 Accepted 12th May 2025

DOI: 10.1039/d5ra02100f

rsc.li/rsc-advances

Antibiotics were initially discovered for their medicinal applications, however, since their introduction, the usage of antibiotics has expanded beyond clinical settings into various sectors, including agriculture, aquaculture, and animal husbandry. In these fields, antibiotics have often been employed non-judicially, primarily as growth promoters or preventative measures against infections, rather than strictly for therapeutic purposes. This widespread and often indiscriminate use has resulted in significant repercussions for both the environment and public health. The accumulation of antibiotics in soil and water ecosystems has led to alterations in microbial communities, fostering the emergence and proliferation of antibiotic-resistant bacteria (ARB). As these resistant strains circulate through various

Chemical Biology Laboratory, Department of Sericulture, Raiganj University, North Dinajpur, West Bengal 733134, India. E-mail: rittickm98@gmail.com; amitmandal08@gmail.com

† Dedicated to Prof. Amiya Kumar Panda, Department of Chemistry and Chemical Technology, Vidyasagar University, on his 57th birthday in recognition of his significant contributions to Biophysical Chemistry.


Dipanjan Das

Dipanjan Das was born in Raiganj, a town in the Uttar Dinajpur district of West Bengal, India. Growing up in a region known for its cultural richness and natural diversity, he developed a strong passion for life sciences and academic inquiry from an early age. He completed his secondary education at Sudarshanpur Dwarika Prasad Uchha Vidyachakra in Raiganj and pursued his undergraduate degree in Botany at Raiganj

Surenranath Mahavidyalaya, affiliated with the University of Gour Banga. He went on to earn his M.Sc. in Botany from Raiganj University, where he refined his research abilities and deepened his expertise in plant biology and related disciplines. Following his post-graduation, Dipanjan qualified several of India's most competitive national examinations. In 2022, he achieved an impressive All India Rank (AIR) of 209 in the CSIR-NET Life Sciences exam, securing the prestigious Junior Research Fellowship (JRF). That same year, he also qualified the GATE examination in Life Sciences. Currently, Dipanjan is pursuing his PhD in the Department of Sericulture at Raiganj University. His future research will focus on the detection of residual antibiotics in sericulture-based products, aiming to enhance product safety, quality control, and consumer health standards within the silk industry and allied sectors.


Joydeep Chakraborty

Dr Joydeep Chakraborty is a dedicated microbiologist specializing in antimicrobial resistance, novel therapeutics, and computational drug discovery. He earned his PhD in Microbiology from Raiganj University in 2024, following a Gold Medal-awarded M.Sc. in Microbiology from the University of North Bengal. With a strong interdisciplinary foundation, Dr Chakraborty's research integrates computa-

tional and experimental approaches. His expertise includes in silico drug target identification, computer-aided drug design (CADD), and the investigation of bacterial ion channels. His work contributes significantly to the fields of drug repurposing, pathogen diagnostics, and translational microbiology. Dr Chakraborty has published extensively in top-tier peer-reviewed journals and co-authored several book chapters on emerging topics such as CRISPR-based detection systems and bioactive microbial compounds. His research continues to address critical global health challenges, with a strong focus on infectious disease management and antimicrobial stewardship.



environmental pathways, they pose a growing threat not only to animal health but also to human health. Thus, the need for rapid, highly sensitive, and affordable detection platforms for ARB diagnostics has become urgent. Up to now, many analytical methods have been reported for the determination of antibiotics, such as HPLC, LC-MS, GC-MS, capillary electrophoresis-MS, etc. But these techniques are expensive, time-consuming, and demand trained operators. The aptamer based biosensors circumvent these problems and could ensure fast on-site analysis of antibiotics. In this review, we discuss how nucleic acid aptamer functionalized nanoparticles emerged as a sanguine answer to overcome the limitations of traditional detection modalities. Moreover, the latest advancement in the development of lateral flow assay, colorimetric, chemiluminescent, surface plasmon resonance, fluorescence and electrochemical biosensors for antibiotics detection have also been explored.

1 Introduction

Antibiotic-resistant microorganisms are a global concern, contributing to a wide range of infectious diseases like cholera, tuberculosis, malaria, and leprosy. These conditions pose significant public health challenges, leading to high rates of morbidity and mortality in both adults and children. The situation is particularly alarming in the case of developing countries, where these challenges are even more pronounced.^{1,2} After, the discovery of antibiotics in the early 20th century the treatment of these diseases became much easier, and many modern medical procedures became possible.³ Antibiotics, useful in inhibiting or killing microorganisms, are essential not

only for human and animal health but also in non-medical applications.⁴ Global antibiotic production has risen significantly within the last few years, with estimates suggesting 100 000 to 200 000 tons annually.^{5,6} In India, antibiotic consumption rate rose sharply from 2000 to 2018.⁷ The excessive and improper use of antibiotics in both humans and animals has led to the rise of antibiotic-resistant bacteria (ARB), posing a global health threat. This overuse has resulted in increased antibiotic excretion into the environment, which in turn promotes the ARB proliferation.⁸ Water soluble antibiotics, in particular, have the capacity to disperse rapidly across aquatic and terrestrial ecosystems, thereby impacting ecological balance and posing considerable risks to both environmental and human health.⁹ Moreover, resistant bacteria and resistance



Pankaj Mandal

Mr Pankaj Mandal is a dedicated researcher in sericulture, originally from Gajol, Malda district, West Bengal. He began his academic journey at Gazole Sewchand Parameswari Vidya-mandir (H.S.) and went on to earn his B.Sc. and M.Sc. degrees in Sericulture from Raiganj University, where he developed a strong foundation in sericultural biotechnology and sustainable practices. Currently pursuing his PhD in the Department of Sericulture at Raiganj University, Mr Mandal is engaged in research that bridges traditional sericulture with modern biotechnological approaches. His academic path reflects a consistent focus on innovation and sustainability in silk production. His future research aims to explore antimicrobial compounds from actinomycetes, targeting pathogens that affect silkworm health. This work holds potential for advancing eco-friendly disease management in sericulture and discovering novel bioactive agents with broader agricultural and pharmaceutical applications. Through this interdisciplinary approach, Mr Mandal seeks to contribute to sustainable rural development and microbial biotechnology.

of Sericulture at Raiganj University, Mr Mandal is engaged in research that bridges traditional sericulture with modern biotechnological approaches. His academic path reflects a consistent focus on innovation and sustainability in silk production. His future research aims to explore antimicrobial compounds from actinomycetes, targeting pathogens that affect silkworm health. This work holds potential for advancing eco-friendly disease management in sericulture and discovering novel bioactive agents with broader agricultural and pharmaceutical applications. Through this interdisciplinary approach, Mr Mandal seeks to contribute to sustainable rural development and microbial biotechnology.



Rittick Mondal

Mr Rittick Mondal was born in Bauria, Howrah, West Bengal. He completed his schooling at Burikhali (K.M.) Institution in his hometown. Rittick earned his Bachelor of Science (B.Sc.) and Master of Science (M.Sc.) degrees in Microbiology from Vidyasagar University, West Bengal, in 2016 and 2018, respectively. He achieved the highest distinction in his M.Sc. program and was awarded a gold medal by Vidyasagar

University in 2019. After completing his M.Sc., Rittick passed the ICAR-NET exam in Agricultural Microbiology in 2018 and enrolled in the PhD program in the Chemical Biology Laboratory, Department of Sericulture, at Raiganj University. In 2021, he was selected as a DST-INSPIRE Junior Research Fellow (JRF), which enabled him to pursue his doctoral research. Rittick currently holds the position of DST-INSPIRE Senior Research Fellow (SRF) in the same laboratory, working under the mentorship of Dr Amit Kumar Mandal, Assistant Professor in the Department of Sericulture at Raiganj University. To date, Rittick has authored over 30 publications in reputable journals, including those from Nature Portfolio, Elsevier, RSC, and ACS. His future research will focus on the development of lateral flow assays and point-of-care diagnostic devices, aiming to improve accessibility to rapid, accurate, and cost-effective diagnostic tools in healthcare and sericulture-related industries.



genes can enter the food chain, leading to infections that are increasingly refractory to conventional treatment.¹⁰ Despite ongoing global research efforts, antibiotic resistance continues to spread. To tackle this crisis, a comprehensive strategy is needed, addressing the overuse of antibiotics and their environmental dissemination. If left unchecked, AMR is projected to cause up to 10 million deaths annually by the year 2050.¹¹ Organizations like the FDA, WHO, and FAO have established maximum residue limits (MRL) to monitor antibiotic levels in food, aiming to limit excessive use and reduce potential health risks (Table 1).¹⁰ To effectively monitor antibiotic contamination in the environment, the development and implementation of highly sensitive and selective detection methods are essential. Such analytical approaches are critical for accurately assessing the presence and concentration of antibiotic residues, thereby enabling timely intervention and informed strategies to mitigate their ecological and public health impacts. Although traditional analytical techniques, such as HPLC,^{12–15} GC-MS,¹⁶ LC-MS/MS,^{17–20} and capillary electrophoresis^{21,22} they present notable limitations. These methods are often cost-prohibitive, require sophisticated instrumentation and trained personnel, and may struggle to distinguish structurally similar antibiotic compounds. Additionally, the presence of certain additives can interfere with analyses and potentially damage sensitive

equipment.¹⁰ In parallel, microbiological techniques and enzyme-linked immunoassays (ELISA), though more accessible and simpler to perform, are prone to false positives and typically involve longer detection times. Taken together, these challenges underscore the urgent need for innovative, rapid, sensitive, and cost-effective detection technologies to facilitate effective environmental monitoring of antibiotic contamination and help mitigate the spread of antibiotic resistance. Aptamer-based biosensors have emerged as a powerful and innovative alternative to conventional antibiotic detection methods, offering significant potential to transform environmental and food safety monitoring while contributing to efforts against antimicrobial resistance (AMR).^{10,23–26} Aptamer are short DNA or RNA molecules (20–80 nt) that specifically bind to target molecules, such as antibiotics, proteins, whole cell bacteria, heavy metals, *etc.*²⁷ These molecular recognition elements underpin the exceptional performance of aptamer-based biosensors, which are characterized by their high sensitivity, selectivity, and stability. Unlike traditional detection approaches, aptasensors enable rapid, on-site analysis with minimal sample preparation and reduced susceptibility to matrix interference, thus overcoming common challenges such as false positives and complex instrumentation requirements.^{28–30} Recent advancements underscore the versatility and effectiveness of aptamer-based biosensing platforms. For example, Liu *et al.* developed a colorimetric aptasensor that achieved an ultra-low detection limit of $4.13 \times 10^{-12} \mu\text{M}$ for kanamycin in milk, utilizing nicking enzyme-assisted signal amplification.³¹ Likewise, Zhou *et al.* employed a catalytic hairpin assembly with G-quadruplex displacement to detect tetracycline with high sensitivity (LOD – $1.035 \times 10^{-2} \mu\text{M}$), applicable to various food matrices.³² More recently, Li *et al.* introduced a label-free fluorescent aptasensor for enrofloxacin with an LOD of $1.58 \times 10^{-4} \mu\text{M}$, integrating a G-quadruplex structure and SYBR Green I dye.³³ while Mohammadi *et al.* reported an electrochemical sensor for tetracycline with a detection limit as low as $1.2 \times 10^{-4} \mu\text{M}$ using AuNPs-modified carbon nanofibers.³⁴ Additionally, Ou *et al.* developed a lateral flow assay based aptasensor capable of detecting kanamycin residues in milk and honey with a visual threshold of 50 nM and a quantifiable LOD of $4.96 \times 10^{-3} \mu\text{M}$.³⁵ Collectively, these recent studies highlight not only the rapid improvement in sensitivity and selectivity of aptamer platforms but also their adaptability for field-use diagnostics. This review consolidates such recent innovations, compares their methodological attributes, and identifies emerging opportunities for future development in real-world diagnostic applications.



Amit Kumar Mandal

Dr Amit Kumar Mandal, born in Kharagpur, West Bengal, India, is a distinguished academic and leading researcher in chemical biology and nano-omics. He currently heads the Centre for Nanotechnology Science (CeNS) at Raiganj University. Dr Mandal completed both his M.Sc. and PhD at the University of North Bengal and previously served as a faculty member at Vidyasagar University under the UGC-Innovative Programme. With

over a decade of experience in research, teaching, and academic leadership, he has authored more than 80 peer-reviewed SCI publications, holds three research patents, and has a cumulative impact score exceeding 400, as recorded by the Web of Science. He actively contributes to the global scientific community through editorial and peer-review roles with leading publishers including Nature Portfolio, RSC, ACS, Wiley, Elsevier, and BioMed Central. A recipient of the prestigious MRSC title, Dr Mandal has earned multiple accolades, including the highly cited review published by RSC & IOP Publishing Top Cited Papers India Award (2022). He is ranked among the top 0.5% of global scholars (ScholarGPS) and among the top 3% of biological scientists in India (AD Scientific Index, 2024). His future research focuses on nano-enabled drug delivery systems, biosensors, and molecular diagnostics aimed at combating infectious diseases, and antimicrobial resistance. These projects are supported by DST-SERB and other national funding agencies.

2 The environmental fate of antibiotics and their effects

To safeguard the health of both humans and animals, antibiotics are extensively utilized across multiple sectors, including agriculture, aquaculture, and healthcare.³⁶ Despite their widespread application, a substantial fraction of administered antibiotics is not fully metabolized and is subsequently released into the environment, contributing to ecological



Table 1 Country wise maximum residue limits (MRLs) of antibiotic

Antibiotics	Product	Detection object	MRL ($\mu\text{g kg}^{-1}$)				
			The EU	Japan	USA	China	
Gentamicin	Pig	Muscle	50	100	100	100	
		Fat	50	100	400	100	
		Liver	200	2000	300	2000	
	Chicken	Kidney	750	5000	400	5000	
		Tissue	—	—	100	100	
		Muscle, fat	100	40	100	100	
Kanamycin	Pig	Liver	600	40	—	—	
		Fat	100	40	—	100	
		Muscle	100	40	—	100	
	Chicken	Liver	600	900	—	600	
		Kidney	2500	4000	—	2500	
		Egg	—	500	—	—	
Neomycin	Cattle	Muscle	500	500	1200	500	
		Milk	1500	2000	150	1500	
		Egg	500	500	—	500	
Streptomycin/dihydrostreptomycin	Cattle, pig, chicken	Kidney	5000	10 000	7200	9000	
		Milk	200	200	—	200	
		Liver, muscle, fat	500	600	500	600	
	Sheep	Kidney	1000	1000	2000	1000	
		Muscle	500	600	600	600	
		Liver	500	600	600	600	
Tetracycline/oxytetracycline/chlortetracycline	Cattle	Kidney	10 000	1000	1000	1000	
		Milk	—	—	200	—	
		Muscle, fat	100	—	200	—	
	Poultry	Liver	600	—	600	—	
		Kidney	1200	—	1200	—	
		Muscle	200	—	200	—	
	Sheep	Liver	600	—	600	—	
		Kidney	1200	—	1200	—	
		Milk	100	—	100	—	
	Swine	Muscle	Muscle	200	—	—	—
			Liver	600	—	—	—
			Kidney	1200	—	1200	—
Turkey		Muscle	200	—	—	—	
		Liver	600	—	—	—	
		Kidney	1200	—	—	—	
Doxycycline	Fish	Muscle	200	—	—	—	
		Liver	600	—	—	—	
		Kidney	1200	—	—	—	
	Lobster	Muscle	200	—	—	—	
		Egg	400	—	—	—	
	Giant pawn	Muscle	200	—	—	—	
		Honey	300	—	—	—	
		Skin and fat	300	—	—	—	
	Cattle, swine, poultry	Muscle	Muscle	100	—	—	—
			Liver	300	—	—	—
			Kidney	600	—	—	—
		Finfish	Fillet	—	—	50	—
Muscle			50	—	50	—	
Muscle			—	—	50	—	
Ampicillin Benzylpenicillin	Cattle	Muscle	—	—	50	—	
		Liver	—	—	50	—	
		Kidney	—	—	50	—	
	Chicken	Milk	—	—	4	—	
		Muscle	—	—	50	—	
		Liver	—	—	50	—	
Kidney	Muscle	—	—	50	—		
	Liver	—	—	50	—		



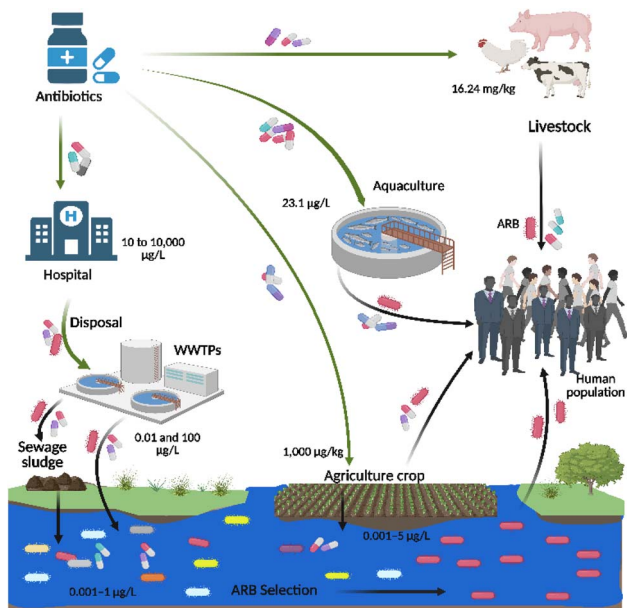


Fig. 1 Discharge of antibiotic residues into the environment and the risks of ARB exposure to humans.

contamination. Research on this topic has progressively increased from 2011 to 2020, reflecting the growing global recognition of environmental antibiotic contamination as a critical concern. Antibiotics can enter the environment through various routes, including their use as feed additives in livestock and aquaculture, agricultural runoff, waste water effluents, the administration of human and veterinary medications, and unregulated environmental discharges from production processes (Fig. 1).⁹

Antibiotics were originally developed to treat diseases but later became widely used as feed additives in animal production. This growing reliance on antibiotics is primarily driven by the increasing demand for high-quality dairy and poultry products. Commonly used antibiotics in animal feeds are tetracyclines, penicillin, chloramphenicol *etc.*^{37,38} In aquaculture, extensive antibiotic use has led to a substantial accumulation of antibiotics in aquatic environments.³⁹ Frequently, used antibiotics in aquaculture are oxytetracycline, chloramphenicol, sulphonamide, amoxicillin *etc.*⁴⁰ In agriculture, the demand for high-quality vegetables has led farmers to spray crops with antibiotics to prevent diseases and enhance crop yields.⁴¹ Commonly used antibiotics in agriculture include streptomycin, oxytetracycline, gentamicin, and oxolinic acid.^{42–44} These practices result in the accumulation of antibiotic residues in soil, water, and crops, often at concerning concentrations. For instance, hospital effluents can contain up to 10 000 $\mu\text{g L}^{-1}$ of antibiotics like ciprofloxacin, amoxicillin while municipal wastewater and WWTP effluents range between 0.01–100 $\mu\text{g L}^{-1}$ and 0.001–5 $\mu\text{g L}^{-1}$, respectively. Manure and poultry waste have been found to contain up to 1000 $\mu\text{g kg}^{-1}$ and 16.24 mg kg^{-1} of antibiotics, respectively, and even vegetables show residues between 6–27 $\mu\text{g kg}^{-1}$.^{45–50} These residual antibiotics persist in the environment and exert selective pressure that

fosters the development and spread of antibiotic-resistant bacteria (ARB) and antibiotic resistance genes (ARGs).⁵¹ Bacteria can acquire antibiotic resistance through two primary mechanisms: the generation of ARGs *via* spontaneous mutations, and the acquisition of ARGs from other microorganisms through horizontal gene transfer (HGT). HGT plays a critical role in the spread of antibiotic resistance among bacterial populations, complementing the spontaneous mutations that generate antibiotic resistance genes (ARGs). While vertical gene transfer (VGT) transmits genetic traits from parent to offspring, HGT enables bacteria to acquire resistance traits directly from other organisms, often across species or genera. This process significantly enhances the genetic plasticity of microbial communities and accelerates the dissemination of ARGs in diverse environments. HGT occurs through three main processes: transformation, where bacteria uptake exogenous DNA, transduction, where bacteriophages mediate genetic transfer and conjugation, which involves the direct exchange of DNA between cells *via* pili. These mechanisms are particularly concerning in the context of environmental antibiotic contamination, as they facilitate the rapid evolution and spread of antibiotic-resistant bacteria (ARB) in soil, water, and agricultural systems—amplifying the public health risks associated with antimicrobial resistance. For example, up to 3% of the *Pseudomonas aeruginosa* genome contributes to its natural resistance. In *Helicobacter pylori*, the mutation rate for resistance to ciprofloxacin and rifampin is between 1×10^{-8} and 2×10^{-8} per cell division.⁵² Most antimicrobials consumed by humans and animals are broken down into their active components. However, a small percentage of these compounds remain constant *i.e.*, still active, in the faeces, which poses a threat to urban wastewater, manure, and biosolids.^{53,54} The use of sewage sludge, manure, biosolids, sediment, and reclaimed water contaminated with antimicrobials for fertilization and irrigation has led to the introduction of antibiotics and bioactive metabolites into water and agro-ecosystems, where they have accumulated in various forms.^{55–57} Environments in the vicinity of livestock farms, aquaculture area, pharmaceutical plants and treated hospital wastewater zones are persistently impacted to antibiotic pollutant. As a consequence of this exposure, antimicrobial levels endure in the environment at differential intensities.⁵⁸ Both aquatic and terrestrial non-target creatures can be negatively impacted by these antibiotic residues.^{59,60} Higher levels of antibiotics can impede plant growth, germination, photosynthesis, and other physiological processes.^{61,62} These residues can impact human health by causing allergic reactions, and abnormalities in the composition of the natural gut bacteria when people consume polluted water and agricultural products.⁶³

Previous studies showed that antibiotics use can change the make-up of the gut microbiota, leading to the rise of opportunistic infections and antibiotic-resistant bacteria.⁶⁴ Such disruptions have been associated with a range of health issues, including Intestinal diseases, pseudomembranous colitis, and an increased risk of colorectal cancer.⁶⁵ Additionally, imbalances in gut microbial communities can impair the development and regulation of the immune system.^{66,67} Environmental



Table 2 Specific aptamer sequences of several antibiotics and their secondary structure (predicted through the Mfold online portal; the portal for the mfold web server is <https://www.unafold.org/mfold/applications/dna-foldingform.php>)⁸⁸

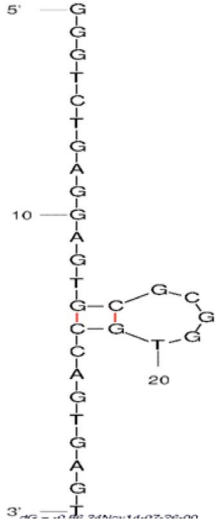
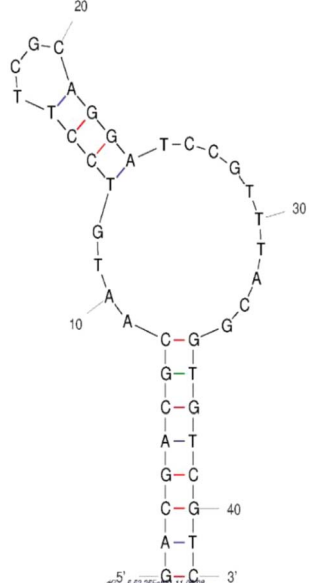
Antibiotics	Aptamer	Length	K_d (nM)	Structure	Reference
Benzylpenicillin	GGGTCTGAG GAGTGCGCGGTGCCAGTGAGT	30	384.3		89
Tetracycline	GACGACGCAATGTCCT TCGAGGATCCGTTTACGGTGTGCGTC	40	62 ± 20		90



Table 2 (Contd.)

Antibiotics	Aptamer	Length	K_d (nM)	Structure	Reference
Tobramycin	CGTCGACGGATCCA TGGCACGTTACAGGTCGACG	34	56.8		91
Sarafloxacin	CTCCGTGCGATCG CCGGGGACCGAAGAATC G'ITCACATCG	40	48.08		92
Chlortetracycline	GGGAUCAUCACA GUGAAAAAAGAUCAC ACUGAAAAAAGAUC	43	2100		93



Table 2 (Contd.)

Antibiotics	Aptamer	Length	K_d (nM)	Structure	Reference
Kanamycin A	TGGGGGTTGAGG CTAAGCCGA	21	78.8		94
Doxycycline	GACGACAAAGCG TTCTACGTGCATA CTTTTGTGGTCGTC	40	490 ± 110		90
Chloramphenicol	CGACATAGAG GATCCATCTTGG GGTGTGTAGTGTGTCG	38	9.8 ± 0.5		81



Table 2 (Contd.)

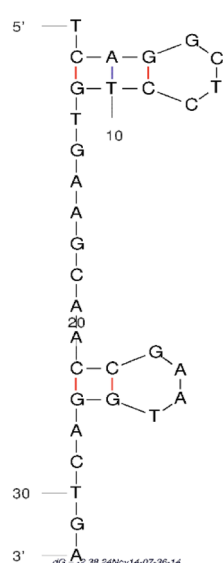
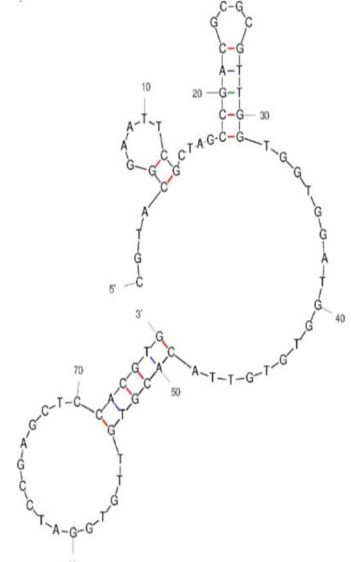
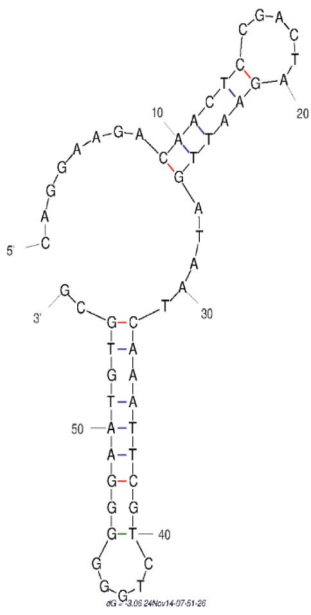
Antibiotics	Aptamer	Length	K_d (nM)	Structure	Reference
Danofloxacin	UCAGGCUCCUGU GAAGCAACCGA AUGGACUGA	32	1.81		97
Oxytetracycline	CGTACGGAATTCG CTAGCCGACGCGCG TTGGTGGTGGATGGT GTGTTACACGTGTTGT GGATCCGAGCTCCACGTG	76	9.61 ± 0.3		98



Table 2 (Contd.)

Antibiotics	Aptamer	Length	K_d (nM)	Structure	Reference
Azlocillin	CAGGAAGACAA CTCGACTAGAATT GATAATCAAATT CGTCTGGGGGGAA TGTGCG	58	55		99

contamination with antibiotics, even at sub-inhibitory concentrations, poses a serious threat to both human and ecological health by fostering the selection and persistence of resistant microorganisms.

3 Progress in aptamer-based antibiotic detection

Aptamers were first discovered in 1990 by Tuerk and Gold, who found RNA sequences that could bind to T4 polymerase using the Systematic Evolution of Ligands by Exponential Enrichment (SELEX) method.^{68,69} In the same year, Ellington and Szostak coined the term “aptamer”, combining the Latin word “*aptus*” (meaning “to fit”) and the Greek word “*meros*” (meaning “part”). In 1992, Ellington and his colleagues expanded their work by selecting the first DNA aptamers that could bind specifically to organic dyes.^{70–72} The systematic SELEX process, which is a patented *in vitro* selection technique, is the cornerstone for identifying aptamers.⁶⁸ During SELEX, a vast library of nucleic acid sequences, each with random sequences arrangement, is screened to find those that specifically bind to a particular target can range from proteins to small molecules, or even entire organisms like viruses and bacteria.⁷³ Once identified, these aptamers can be further modified for a variety of applications, particularly in biosensing both *in vitro* and *in vivo*. SELEX has evolved over the years with numerous modifications, such as negative SELEX and counter SELEX, to enhance the specificity and efficiency of aptamer selection. Special techniques like capture-SELEX and nanomaterial-based SELEX have proven especially useful for selecting aptamers targeting

small molecules, including antibiotics.^{74,75} To improve their stability and make them more suitable for biosensing applications, aptamers are often chemically modified at both ends.⁷⁶ These modifications enhance their resistance to nucleases (enzymes that degrade nucleic acids), allowing the aptamer to remain stable over time. Aptamers like other nucleic acid sequences can adopt a variety of secondary and tertiary structure including hairpins, stem-loops, bulges, pseudoknots, i-motifs, and G-quadruplexes which underpin their ability to bind target analytes with high specificity and affinity.^{73,77} These structures enable aptamers to bind to their targets selectively through electrostatic interactions, hydrogen bonds or van der Waals forces. The binding affinity between aptamer and its target is typically quantified by the dissociation constant (K_d), which measures how tightly the aptamer binds. A lower K_d indicates a stronger interaction, with values typically ranging from picomolar (pM) to micromolar (μ M) concentrations, depending on the specific target.⁷⁶ While RNA aptamers were the first to be discovered and offer complex 3D structures, DNA aptamers are now preferred in many applications due to their enhanced stability, resistance to degradation, and simpler SELEX process, which doesn't require reverse transcription.^{78,79} Antibodies have long been employed in biosensing due to their high specificity and strong binding affinity to biological targets; however, their practical use is often constrained by high production costs, limited stability, and shorter shelf life. In contrast, aptamers present several distinct advantages over antibodies, including cost-effective synthesis, superior thermal and chemical stability at room temperature, extended shelf life, and reusability. Additionally, aptamers can be engineered to



Review

recognize non-immunogenic targets—such as antibiotics and metal ions which are typically challenging for antibodies to detect with high efficiency.³⁰

Numerous antibiotic aptamers with strong binding affinities to their targets have been developed, as summarized in Table 2. However, not all aptamers are as reliable as initially thought. For example, early studies revealed that some antibiotic aptamers, like those for ampicillin, did not exhibit effective binding in assays like isothermal titration calorimetry (ITC).⁸⁰ Similarly, chloramphenicol (CAP) aptamers showed poor binding in ITC assays, suggesting that they, like the ampicillin aptamers, may not have been true aptamers for their intended antibiotic targets.⁸¹ These findings underscore the critical need for rigorous characterization of aptamer–target interactions to confirm their authenticity and functional reliability. To overcome limitations observed with earlier aptamers, Zhao *et al.* employed modified SELEX techniques, such as capture-SELEX, to successfully develop new high-affinity DNA aptamers, including those specifically targeting chloramphenicol (CAP).⁸² The success of these innovations has been supported by global research efforts that continue to advance aptamer screening techniques and expand their applications in biosensing.⁸³ For example, to screen the enrofloxacin (ENR) aptamer using Fe³⁺-IDA beads, Choe *et al.* used capillary electrophoresis and typical SELEX techniques.⁸⁴ Using lomefloxacin as the target molecule and polydopamine magnetic nanobeads as separation carriers, Liu *et al.* developed a new aptamer screening method enabled by magnetic separation, exhibiting excellent specificity to lomefloxacin with little affinity for the structurally related molecules of ofloxacin, ENR, and norfloxacin.⁸⁵ Additionally, You *et al.* developed a functionalized graphene-based approach was used to assess the ofloxacin DNA aptamer using the standard SELEX methodology, representing good affinity and specificity to ofloxacin. They are commonly used in the construction of diverse sensing devices. Biosensing devices' sensitivity is enhanced using nanomaterials with distinct physical and chemical properties, such as stability, large surface area, and excellent electrical/optical performance. These include metal oxide nanoparticles, carbon nanotubes, graphene, oxidized graphene, quantum dots, and gold nanoparticles (AuNPs), all of which improve detection efficiency.^{86,87}

4 Implementation of aptasensors for antibiotics detection

4.1. The colorimetric aptasensor

Colorimetric methods provide a visually interpretable signal output, enabling the detection of target analytes through distinct color changes that can be assessed either by the naked eye or using simple, cost-effective portable devices. These methods are particularly advantageous for rapid screening and point-of-care (POC) diagnostics.^{100–102} Metallic nanomaterials such as gold nanoparticles (AuNPs), silver nanoparticles (AgNPs), and magnetic particles are extensively utilized in colorimetric sensing due to their unique optical properties, which are modulated by particle size, shape, and interparticle

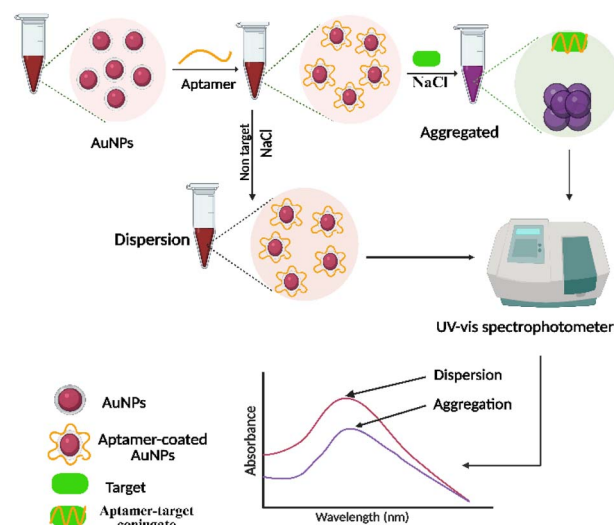


Fig. 2 Colorimetric aptasensor for antibiotic detection using AuNPs.

distance.¹⁰³ These tunable optical characteristics enhance both the sensitivity and versatility of the sensing platform across diverse analytical applications, without necessitating sophisticated instrumentation.¹⁰¹ Aptamers are frequently employed as biorecognition elements in colorimetric aptasensors due to their high affinity, specificity, and structural adaptability. They can non-covalently adsorb onto the surfaces of metallic nanoparticles *via* electrostatic interactions, allowing the monitoring of binding-induced changes through visual cues or ultraviolet-visible spectroscopy.^{104–106} Among various nanomaterials, AuNPs-based aptasensors have gained particular attention for antibiotic detection owing to their high extinction coefficients, excellent biocompatibility, and pronounced localized surface plasmon resonance (LSPR) effects.^{107,108} The typical AuNPs based colorimetric sensing mechanism relies on aggregation-induced LSPR shifts. In the absence of the target, AuNPs are stabilized by aptamers or double-stranded DNA (dsDNA), preventing salt-induced aggregation and maintaining a stable red colloidal dispersion. Upon target introduction, aptamer binding causes structural changes or detachment from the nanoparticle surface, leading to aggregation under salt conditions and producing a visible red-to-blue color transition. This aggregation-induced optical change forms the basis for both qualitative visual detection and quantitative measurement *via* UV-vis absorbance analysis (Fig. 2).¹⁰⁹

Additionally, AuNPs can act as peroxidase-mimicking nanozymes, catalyzing hydrogen peroxide-mediated chromogenic reactions that further improve detection sensitivity.¹¹⁰ Several studies have successfully applied these principles for antibiotic residue detection. For example, Song *et al.* developed a AuNP-based aptasensor for kanamycin (KAN) detection, using single-stranded DNA (ssDNA) aptamers to regulate nanoparticle aggregation. In the presence of KAN, aptamer binding caused aggregation of AuNPs, resulting in a visible color shift and a detection limit (LOD) of 0.025 μM .¹¹¹ Xu *et al.* constructed a similar aptasensor using AgNPs, wherein the aptamer KAN



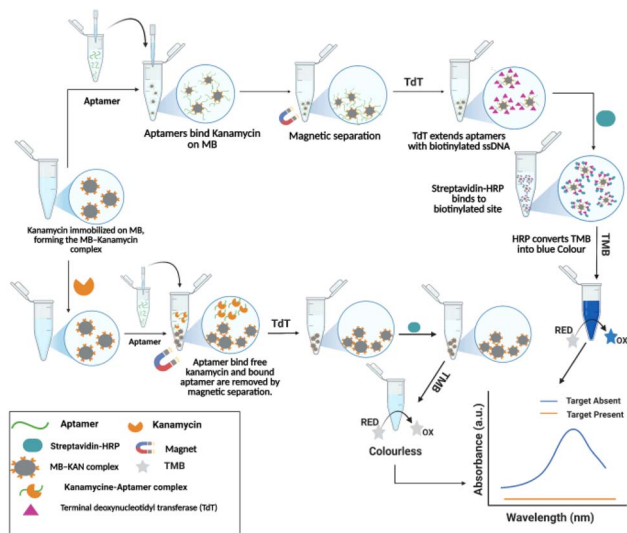


Fig. 3 Magnetic particle-based colorimetric aptasensor utilizing terminal deoxynucleotidyl transferase for kanamycin detection.

interaction induced nanoparticle aggregation and a measurable color change, achieving a LOD of $5.37 \times 10^{-3} \mu\text{M}$ within 20 minutes.¹¹² Ha *et al.* reported a user-friendly paper-based colorimetric assay using wax-printed chips and AuNPs for ultra-sensitive KAN detection. This platform enabled visual detection of KAN concentrations as low as $3.35 \times 10^{-3} \mu\text{M}$, providing a low-cost, field-deployable solution.¹¹³ Another study of colorimetric aptasensors based on magnetic particles represent a robust and versatile strategy for the sensitive and selective detection of analytes in complex sample matrices. In these systems, aptamer-functionalized magnetic particles specifically bind the target, and magnetic separation removes unbound components, minimizing background interference. Visual signal generation is achieved through the use of colorimetric probes such as AuNPs and horseradish peroxidase (HRP). AuNPs function as optical indicators, exhibiting a red color when stabilized in their dispersed state by aptamers, and transitioning to blue upon aggregation induced by analyte binding through salt or hybridization effects. In parallel, enzyme-linked probes such as HRP catalyze the oxidation of chromogenic substrates like 3,3',5,5'-tetramethylbenzidine (TMB), producing a distinct and quantifiable colorimetric response. Building on this concept, Zhao *et al.* developed a competitive colorimetric aptasensor for KAN detection incorporating terminal deoxynucleotidyl transferase (TdT) mediated signal amplification. In the absence of KAN, aptamers bind to KAN functionalized magnetic beads (MBs-KAN), enabling TdT to catalyze biotin dUTP incorporation into extended ssDNA. This biotinylated DNA binds streptavidin-horseradish peroxidase (SA-HRP), which triggers a chromogenic reaction. However, in the presence of KAN, aptamers preferentially bind the free antibiotic, preventing MBs binding, TdT extension, and color development. The sensor achieved a low LOD of $9 \times 10^{-6} \mu\text{M}$ and exhibited high analytical accuracy (Fig. 3).¹¹⁴

A more advanced multiplexed colorimetric aptasensor was developed by Du *et al.*, employing a sandwich design with split aptamers immobilized on AuNPs and MBs. Upon target binding, aptamer reconstitution enabled magnetic separation and analyte enrichment. TdT then generated polyadenine sequences at the 3'-ends, which served as primers for rolling circle amplification (RCA). The RCA product hybridized with an HRP-labeled DNA probe, catalyzing tetra methyl benzidine (TMB) oxidation in the presence of H_2O_2 to yield a blue signal. This system enabled simultaneous detection of enrofloxacin (ENR), For ENR, the LOD was $6.96 \times 10^{-12} \mu\text{M}$ in fish.¹¹⁵ Liu *et al.* further enhanced sensitivity by integrating nicking enzyme-assisted signal amplification with aptamer recognition. In this design, a hairpin aptamer unfolded upon binding KAN, facilitating signal amplification *via* platinum-labeled probes and MBs, achieving an ultra-low LOD of $4.13 \times 10^{-12} \mu\text{M}$ in milk.³¹ For tetracycline (TC), Zhang *et al.* utilized gold nano-clusters with intrinsic peroxidase-like activity in a colorimetric platform, detecting TC at concentrations as low as $0.5 \mu\text{M}$ with a LOD of $4.60 \times 10^{-2} \mu\text{M}$, showing high selectivity in real samples such as milk.¹¹⁶ In another approach, Wang *et al.* developed a label-free colorimetric aptasensor using a 40-mer T-rich aptamer, achieving a LOD of $2.79 \times 10^{-2} \mu\text{M}$ and enabling visual detection of TC in honey.¹¹⁷ Other notable examples include a microplate-based sensor for tilmicosin with a LOD of $1.0 \mu\text{M}$.¹¹⁸ Furthermore smartphone integrated POC assay for streptomycin (STR) utilizing SYBR Green I and aptamers, yielding a LOD of $9.40 \times 10^{-2} \mu\text{M}$.¹¹⁹ These advancements illustrate the broad potential and adaptability of aptamer-based colorimetric assays for antibiotic residue monitoring in food safety and environmental applications.¹¹⁹ Further antibiotic detection using colorimetric aptasensors summarized in Table 3. Their high specificity, ease of fabrication, and user-friendliness make them ideal for high-throughput screening, food and environmental analysis, and label-free detection.^{96,120} Colorimetric techniques usually rely on homogeneous solution systems, which can be influenced by environmental factors during real sample analysis, potentially affecting accuracy. Additionally, the drawback of colorimetric aptasensors often require a large amount of aptamer, limiting sensitivity, necessitating enhanced signal amplification for improved performance.^{10,120}

4.2. Fluorescence aptasensor

Fluorescence is an exceptionally sensitive optical phenomenon extensively applied in aptamer-based biosensing platform due to its high signal-to-noise ratio and adaptability to real-time detection platforms.¹²¹ As DNA and RNA aptamers inherently lacks intrinsic fluorescence, they must be conjugated with external fluorophores or fluorescent nanomaterials to enable fluorescence-based sensing.¹²² Fluorescent aptasensors are generally categorized into two main formats: labeled and label-free systems, each utilizing distinct signal generation and amplification mechanisms.¹²³

Aptamer fluorescence sensing systems often utilize strategies, such as (a) molecular beacon designs where aptamers are



Table 3 Comparative overview of various aptasensors for antibiotic detection^a

Aptasensor	Analytes	Strategy	LOD (μM)	LR (μM)	Signal amplification	Matrix	Reference
Colorimetric aptasensor	KAN	Hairpin aptamer DNA/enzyme cutting signal amplification	4.13×10^{-12}	—	Nicking enzyme-assisted amplification	Milk	31
	KAN	High salt induces AuNPs aggregation from red to blue the catalytic chromogenic reaction of AuNPs mimics	0.025	—	Colour change based on aggregation of AuNPs	Pharmaceutical preparations, food products	111
	KAN	Disrupts AgNPs protective mechanism against salt induced aggregation	5.37×10^{-3}	1.03×10^{-4} to 1.24×10^{-3}	Protection of AgNPs against salt-induced aggregation	Milk	112
	KAN	Paper chip-based, label-free, colorimetric assay using AuNPs and RGB color analysis	3.35×10^{-3}	—	—	Milk	113
	KAN	Competitive recognition between KAN, MBs-KAN, and aptamer with TdT-mediated signal amplification	9×10^{-6}	—	TdT-mediated signal amplification (HRP)	Milk, honey	114
	ENR	MB/SPA	6.96×10^{-12}	2.78×10^{-12} to 2.78×10^{-6}	Aggregation-induced signal change	Fish	115
	TC	Gold nanocluster–ligand–TMB	4.60×10^{-2}	1–16	Enhancement <i>via</i> aptamer recognition	Drugs, milk	116
	TC	Aptamer–AuNPs/NaCl	2.79×10^{-2}	—	—	Honey	117
	TIL	MP/HRP–SPA	1.0	—	Peroxidase-like activity of hybrids	—	118
	STR	SYBR Green, I bind with aptamer DNA fluorescence	9.40×10^{-2}	0.1–100	Peroxidase-like activity enhanced by aptamer binding	Chicken, milk	119
	STR	Aptamer–AuNPs/NaCl	8.60×10^{-2}	0.1–0.5	—	Milk	135
	OFX	Aptamer/AuNPs/NaCl	3.40×10^{-5}	2.00×10^{-2} to 4.00×10^{-1}	—	Aqueous solutions	136
	TC	Aptamer–AuNPs/NaCl/cysteine-stabilized AuNPs	8.79×10^{-5}	4.50×10^{-4} to 4.50×10^{-3}	—	Raw milk	137
	TOB	Unmodified AuNPs and ssDNA	2.33×10^{-2}	4.00×10^{-2} to 2.00×10^{-1}	—	Milk, chicken eggs	138
	OTC	Truncated 8-mer ssDNA aptamer	1.00×10^{-4}	—	—	—	139
	SUL	Peroxidase like activity of Gr/Ni@Pd nanoparticles	2.77×10^{-3}	3.95×10^{-3} to 1.57×10^{-4}	—	Lake water	140
	TC	GO/aptamer's	2.25×10^{-7}	4.50×10^{-7} to 4.50×10^{-4}	GO aggregation, aptamer protection	Honey	141
	KAN	AuNPs enable colorimetric biosensing <i>via</i> , antibiotic adsorption-induced aggregation	9.00×10^{-2}	—	—	—	142
	CIP	AuNPs modified with FQ-binding aptamer and complementary DNA (“flower” structure)	2.6×10^{-3}	—	Catalytic activity of AuNPs reduces 4-nitrophenol	Serum	143



Table 3 (Contd.)

Aptasensor	Analytes	Strategy	LOD (μM)	LR (μM)	Signal amplification	Matrix	Reference
Fluorescence aptasensors	TC	Catalytic hairpin assembly and G-quadruplex displacement	1.035×10^{-2}	0–2.25	Catalytic hairpin assembly and G-quadruplex displacement	Milk	32
	ENR	G-quadruplex DNA aptamer SG-I	1.58×10^{-4}	1.95×10^{-3} to 4.0×10^{-1}	Aptamer and SYBR Green I (SG-I) fluorescence quenching	Chicken, fish, pork samples	33
	PEN	Aptamer selected by rGO-SELEX	9.2×10^{-3}	0.104–4.17	Fluorescence recovery signal from rGO surface	Milk	89
	TC	Fluorescence quenching with aptamers in a THMS	2.09×10^{-3}	—	THMS	Tap water, rat serum	124
	TC	DNA-AgNCs	2.58×10^{-2}	0.0002–0.002 & 0.002–0.8	Aptamer-templated AgNCs	Milk	125
	OTC	Aptamer-conjugated MB and PicoGreen dye	1.5×10^{-4}	0.005–0.25	Aptamer conjugated to magnetic beads and PicoGreen (PG) fluorescent dye	Milk	126
	STR	Fluorescent aptasensor using Exo III and SYBR Gold	5.45×10^{-2}	—	Exonuclease III-assisted target recycling	Milk, blood serum	127
	ENR	SPA assisted MNPs and magnetic separation	2.23×10^{-5}	0–0.6	DNA tweezers fluorescence aptasensor with split aptamer and magnetic separation	Spiked milk samples	128
	ENR	Aptamer, GO and native fluorescence	3.70×10^{-3}	1×10^{-7} to 1.0×10^{-1}	—	Raw milk	129
	ENR	G-quadruplex DNA aptamer SG-I	5.9×10^{-4}	0.04–0.24	—	Food, serum samples	130
	KAN	AuNPs to quench CDs fluorescence <i>via</i> the IFE	1.80×10^{-2}	1×10^{-7} to 1.0×10^{-1}	AuNPs as fluorescence quenchers for CDs	Milk	131
	KAN	Enzyme-free fluorescent aptamer sensor based on EDSDR	5.3×10^{-5}	5×10^{-3} to 5×10^{-2} & 7.5×10^{-2} to 1	EDSDR	Milk	132
	KAN	SPA, DNA-AgNCs, and Exo I for signal amplification	1.07×10^{-3}	—	Exo 1 assisted target recovery amplification	—	133
	KAN	FAM-labeled aptamer and AuNPs for dynamic fluorescence quenching	1.0×10^{-7}	1×10^{-4} to 5×10^{-2}	AuNPs and FAM-fluorescent aptamer quenching <i>via</i> dynamic IFE	Milk	144
	KAN	Amino-functionalized SiO_2 , CuNCs, and DNA-AgNCs	7.3×10^{-3}	5×10^{-3} to 6×10^{-1}	FRET between CuNCs and DNA-AgNCs	—	145
KAN	IFE between AuNPs and GOQDs	3.6×10^{-3}	0.0001–0.1	IFE between AuNPs and GOQDs	Milk, honey, serum	146	
AMP	AuNPs modified MB composites and NEASA	2.0×10^{-4}	2.86×10^{-4} to 2.86×10^{-1}	NEASA	River water	147	
OTC	GO hydrogel, co-crosslinked with adenosine and aptamer	5.43×10^1	5×10^{-6} to 1×10^{-1}	3D hydrogel crosslinked by aptamers and adenosine	—	148	
CAP	FRET assisted by SSB	9.29×10^{-6}	1×10^{-4} to 2×10^{-2}	FRET	—	149	
CAP	Aptamer based detection system combined with qRT-PCR	3.1×10^{-4}	0.1 to 10	—	Milk	150	
NEO	Aptamer-based sensor combined with AuNPs	1.0×10^{-2}	—	Fluorescence quenching by AuNPs	Milk	151	
AMP	Indirect (fluorescent signal <i>via</i> aptamer-analyte binding)	2.06×10^{-2}	1.0×10^{-1} to 1.0×10^2	—	Human urine	152	



Table 3 (Contd.)

Aptasensor	Analytes	Strategy	LOD (μM)	LR (μM)	Signal amplification	Matrix	Reference
Electrochemical aptasensor	ENR	Pb ²⁺ -dependent DNzyme-driven DNA walker with triple amplification, combining AuPt@h-CeO ₂ , PEI-MoS ₂ , and Au@ZnNi-MOF	3.08×10^{-10}	1.51×10^{-8} to 3.03×10^{-3}	DNzyme cleavage, gold nanoparticle-based amplification	Water, milk	153
	ENR	NiCo ₂ O ₄ @NiO	4.65×10^{-11}	1.39×10^{-10} to 1.39×10^{-1}	Composite electrode for enhanced electron transfer	—	154
	ENR	CoCH-6 h/GCE	1.0×10^{-1}	—	Electrode modification for enhanced sensitivity	Pork, meat	155
	TC	GCE modified by CNF and carboxylated MWCNTs/aptamer/molecular docking and CCD	2.28×10^{-12}	1.0×10^{-11} to 1.0×10^{-5}	Molecular docking & multi-walled carbon nanotube modification	Milk	156
	KAN	DNA signal amplification strategy that combines RecJf exonuclease-assisted target recycling and HCR	1.8×10^{-3}	1.0×10^{-2} to 1.0×10^1	RecJf exonuclease and HCR amplification	Milk	157
	KAN	ESDR strategy for the enzyme-free ratiometric electrochemical aptasensor	0.0001526	—	Enzyme-free ratiometric signal amplification	—	158
	STR	MMCM as the loading material immobilized on a MGCE/aptamer	1.5×10^{-5}	1.72×10^{-4} to 1.72×10^1 to 1.72×10^2	Magnetic nanoparticle adsorption and current change	Milk	159
	STR	Pd@Ti ₃ C ₂ -PEI-NCNTs composite	3.0×10^{-6}	1.0×10^{-5} to 7.0×10^{-1}	Pd nanocomposite signal amplification	—	160
	KAN	Aptamer-based target-triggered DNA adsorption on MoS ₂ nanosheets combined with enzymatic amplification	2.9×10^{-5}	—	MoS ₂ nanosheet-based DNA adsorption with enzymatic amplification	—	161
	KAN	HCR strategy combined with magnetic nanoparticle-based aptamer capture	1.0×10^{-6}	1.0×10^{-6} to 1.0×10^{-1}	Magnetic nanoparticle aptamer-based signal detection	Milk	162
	KAN	dsB-TMSDR, enabling dual-signal amplification/HCR is triggered to amplify the signal/MB is used as a redox probe for signal generation	1.6×10^{-5}	—	Dual-signal amplification (TMSDR + HCR)	—	163
	KAN	UiO-66-NH ₂ /MWCNT@rGONR/MCA-based COF	1.3×10^{-2}	2.5×10^{-2} to 9.0×10^{-1}	Nanocomposite for enhanced electrochemical response	Fish, meat, milk	164
	STR	Ti ₃ C ₂ and MOFs nanocomposite	3.3×10^{-6}	1.0×10^{-5} to 2.0×10^{-1}	MOF/TNG nanocomposite for STR detection	Milk	165
	ENR	MNPs as carriers	1.5×10^{-5}	3.0×10^{-5} to 3.0×10^{-1}	Magnetic nanoparticles aptamer-based signal detection	Chicken	166
	TC	Co assembly strategy combining stone-like-AuNPs and N-doped carbon aerogel (NCA)	3.2×10^{-10}	1.00×10^{-9} to 1.00×10^{-5}	N-doped carbon aerogel/AuNPs	Milk	167
	OTC	Signal-on aptasensor <i>via</i> Fc-DNA hairpin switch and target-aptamer competition	Serum: 2.61 ± 0.26 Urine: 1.09 ± 0.15	2.17×10^{-2} to 1.30×10^0	—	Mouse blood serum and urine	168
	AMP	Signal-on aptamer probe with conformational change	$1 (\text{ACV})/30 (\text{SWV})$	—	—	Serum, saliva, milk	169



Table 3 (Contd.)

Aptasensor	Analytes	Strategy	LOD (μM)	LR (μM)	Signal amplification	Matrix	Reference
	DNM	Label-free electrochemical aptasensor with PS & aptamer on AuNP-polyTTBA	$5.23 (\pm 0.21) \times 10^{-5}$	1.0×10^{-4} to 6.0×10^{-2}	Conducting polymer (polyTTBA)	Spiked human urine	170
	GEN	RNA aptamer-based electrochemical sensor; tested methylation, DNA analog, and ultrafiltration	1.5	—	—	Human serum	171
	TOB	Faradaic-EIS displacement assay using fully O-methylated RNA aptamer (FATA)	0.7	3–7.21	—	Human serum	172
Cemiluminescent aptasensor	KAN	Oligonucleotide-based “switch-on” luminescent assay using a Pt(II) complex as signal transducer <i>via</i> aptamer conformational change	143	0.2–150	Luminescence enhancement <i>via</i> intercalation of Pt(II) complex into aptamer hairpin structure	Buffer and fish	173
	KAN	FALIA using CNPs	1.032×10^{-13}	2.06×10^{-13} to 2.06×10^{-16}	Enhanced fluorescence due to photoluminescence properties of CNPs linked with aptamer recognition of kanamycin	Milk	174
	KAN	“On-off-on” switch strategy	4.5×10^{-5}	0.00015–170 000	On-off-on ECL aptasensor with DNzyme-enhanced nanofilm amplification	Aqueous solutions	175
	OTC	ABEI-functionalized gold nanostructures	4.345×10^{-8}	1.085×10^{-7} to 1.085×10^{-5}	ABEI- H_2O_2 -PIP CL system	Milk	176
	TC		4.5×10^{-8}	1.126×10^{-7} to 1.126×10^{-5}			
	KAN		4.13×10^{-9}	1.03×10^{-8} to 1.03×10^{-5}			
SPR aptasensor	KAN	Continuous-flow graphene-based SPR aptasensor utilizing irreversible affinity interaction	2.85×10^{-1}	1–100	π - π interaction between graphene and aptamer enhances immobilization	Milk	177
	TOB	T-LSPR aptasensor with gold nanoislands on fluorine-doped tin oxide (FTO)-coated glass integrated with CMOS sensor	3.4	10–80	Plasmon shift measured by peak wavelength and hue change	Blood serum	178
	NEO	SPR and FIS aptasensor using 2'-O-methyl RNA aptamer for enhanced nuclease resistance	5.0×10^{-3}	0.01–100	—	Buffer	179
LFA aptasensor	KAN	Lateral flow strip biosensor using magnetic microspheres (MMS) and DNA-functionalized AuNPs	4.96×10^{-3}	0.005–0.5	Target-mediated displacement of cDNA; AuNP-DNA hybridization signal	—	35
	OTC	Lateral flow aptasensor with aptamer-AuNP conjugate and OTC-protein conjugate on strip	1.08×10^{-4}	—	Competitive binding between aptamer-AuNP and OTC-protein	Spiked milk	180



Table 3 (Contd.)

Aptasensor	Analytes	Strategy	LOD (μM)	LR (μM)	Signal amplification	Matrix	Reference
	AMP	Competitive lateral flow assay using aptamer-based recognition	1.72×10^{-8}	—	Two aptamers with cross-recognition	Milk	181

^a LOD = limit of detection, LR = linear range, PEI = polyethyleneimine, MoS₂ = molybdenum disulfide, AuPt@h-CeO₂ = gold and platinum-coated hollow cerium oxide, MOF = metal-organic framework, CNF = carbon nanofiber, MWCNTs = multi-walled carbon nanotubes, NCA = N-doped carbon aerogel, rGONR = reduced graphene oxide nanoribbon, MCA = melamine and cyanuric acid monomers, and COF = covalent organic framework, GCE = glassy carbon electrode, CoCH-6 h/GCE = cobalt-based hybrid-modified GCE, MGCE = magnetic glassy carbon electrode, MMCM = magnetic mesoporous carbon materials, Pd@Ti₃C₂-PEI-NCNTs = palladium nanoparticles/titanium carbide/polyethyleneimine-functionalized nitrogen-doped carbon nanotubes, AuPt@h-CeO₂ = gold and platinum-coated hollow cerium oxide, MOF = metal-organic framework, CNF = carbon nanofiber, MWCNTs = multi-walled carbon nanotubes, NCA = N-doped carbon aerogel, rGONR = reduced graphene oxide nanoribbon, MCA = melamine and cyanuric acid monomers, and COF = covalent organic framework, GCE = glassy carbon electrode, CoCH-6 h/GCE = cobalt-based hybrid-modified GCE, and MGCE = magnetic glassy carbon electrode, Gr/Ni@Pd = graphene/nickel/palladium, MMCM = magnetic mesoporous carbon materials, CCD = central composite design, Pd@Ti₃C₂-PEI-NCNTs = palladium nanoparticles/titanium carbide/polyethyleneimine-functionalized nitrogen-doped carbon nanotubes, MNPs = magnetic nanoparticles, MBS = magnetic beads, HCR = hybridization chain reaction, EDS/DR = entropy-driven strand displacement reaction, dSB-TMSDR = double stir bar-assisted toehold-mediated strand displacement reaction, Exo I = exonuclease I, SPA = split aptamer, FRET = fluorescence resonance energy transfer, IFE = inner filter effect, SG-I = SYBR Green I, SSB = ssDNA binding protein, CDs = carbon dots, DNA-AgNCs = DNA-templated silver nanoclusters, AuNPs = gold nanoparticles, GO = graphene oxide, GOQDs = graphene oxide quantum dots, CuNCs = copper nanoclusters, SiO₂ = silica nanoparticles, qRT-PCR = quantitative real-time PCR, NEASA = nicking enzyme-assisted signal amplification, THMS = triple-helix molecular switch, NaCl = sodium chloride, MP = microplate plate, HRP = horseradish peroxidase, KAN = kanamycin, STR = streptomycin, OTC = oxytetracycline, ENR = entrofloxacin, PEN = penicillin, TIL = tilimicosin, TOB = tobramycin, OFX = ofloxacin, CIP = ciprofloxacin, SUL = sulfonamides, NEO = neomycin, AMP = ampicillin, DNM = daunomycin, GEN = gentamicin, CAP = chloramphenicol, TC = tetracycline.

tagged with fluorophore-quencher pairs; (b) fluorescence quenching platforms using aptamer-bound fluorophores in conjunction with carbon nanomaterials; (c) G-rich DNA sequences serving as effective quenchers in fluorophore-tagged aptamer systems; and (d) conformational structures like G-quadruplexes that, upon target interaction, emit or modulate fluorescence signals.⁹⁶ These platforms have been increasingly leveraged for the sensitive and selective detection of antibiotics in food matrices.

Earlier reported study by Jalalian *et al.* introduced a Triple-Helix Molecular Switch (THMS) aptasensor for tetracycline (TC) detection. This system utilized fluorescence quenching upon target binding and achieved a detection limit of 2.09 nM,¹²⁴ laying the groundwork for further innovation in fluorescence sensing. Building upon this, Zhou *et al.* developed an enzyme-free detection method integrating catalytic hairpin assembly (CHA) and G-quadruplex DNA displacement, which demonstrated high sensitivity with a detection limit of 4.6 $\mu\text{g L}^{-1}$, making it suitable for a wide range of sample types.³² Another notable advancement was the development of an aptamer-templated silver nanocluster (DNA-AgNC) biosensor for TC, which achieved a detection limit of 11.46 ng mL⁻¹ and a broad linear range from 20 ng mL⁻¹ to 10 $\mu\text{g mL}^{-1}$.¹²⁵ Similarly, Bahreyni *et al.* constructed a highly sensitive aptasensor for oxytetracycline (OTC) detection by immobilizing OTC-specific aptamers onto magnetic beads and utilizing Pico-Green dye. This system achieved an impressive detection limit of 0.15 nM, with linear ranges spanning 0.2–2 nM and 2–800 nM, demonstrating its suitability for food sample analysis.¹²⁶ The field has further expanded with the emergence of label-free fluorescent biosensors. For example, Taqhdisi *et al.* developed a label-free fluorescence aptasensor for streptomycin detection using exonuclease III, SYBR Gold dye, and a complementary DNA strand. In the absence of streptomycin, the aptamer remained hybridized to the complementary strand, resulting in minimal fluorescence. Upon target addition, the aptamer selectively bound to streptomycin, releasing the complementary strand and preserving the double-stranded DNA from exonuclease III degradation (Fig. 4). This intact DNA was then able to bind SYBR Gold, generating a strong

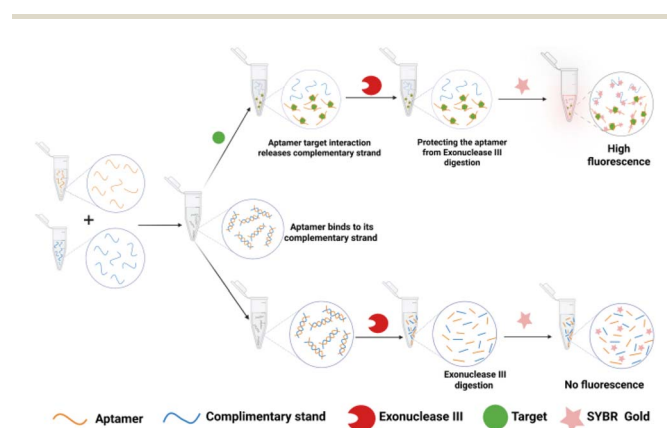


Fig. 4 Schematic illustration of the fluorescence aptasensor for antibiotics detection.

fluorescence signal with a detection limit of $5.45 \times 10^{-2} \mu\text{M}$ in milk and blood samples.¹²⁷

Innovative approaches have also employed DNA tweezers, G-quadruplex DNA, and graphene oxide-based quenchers to further enhance fluorescence output, particularly for the detection of antibiotics such as enrofloxacin (ENR),^{33,128–130} achieving ultra-low detection limits and broad dynamic ranges. In the case of kanamycin (KAN), label free gold nanoparticle (AuNP)-based sensors exploiting the inner filter effect (IFE), entropy-driven strand displacement reactions (EDSDR), exonuclease I digestion strategies, and silver nanocluster templates have all been reported.^{131–133} Dual-mode sensors combining fluorescence and colorimetric outputs now offer real-time analysis with smartphone integration, significantly improving field-deployable diagnostics. These technological advancements underscore the remarkable evolution of fluorescence-based aptasensors—from basic fluorescence quenching systems to highly integrated platforms utilizing nanomaterials such as silver nanoclusters, gold nanoparticles, and carbon quantum dots.^{125,134} Recent progress in dual-mode sensors has enhanced detection versatility and speed, holding promise for real-time monitoring of antibiotic residues in both food and environmental samples. These sensors are employed in various strategies to detect antibiotics, as summarized in Table 3. However, fluorescence aptasensors still face challenges including photobleaching, background fluorescence, and interference from complex matrices, which may compromise sensitivity and specificity under certain conditions.¹²⁰

While current fluorescent aptasensors are predominantly designed for single-target detection, the development of multi-analyte platforms employing multicolor quantum dots offers a promising avenue for simultaneous detection of multiple antibiotic residues. Such multiplexed systems could significantly increase detection throughput and efficiency.^{96,120} Given the global concerns over antimicrobial resistance and the demand for stringent monitoring, fluorescence-based aptasensors are poised to play a pivotal role in enhancing food safety and environmental surveillance.

4.3. Electrochemical aptasensor

Electrochemical biosensors have become vital tools for detecting and measuring various analytes across different fields. These sensors typically consist of an electrode combined with a molecular recognition element and an electrochemically active component. When the target analyte interacts with the recognition element, it induces changes on the surface of the electrode. These changes are then converted into electrochemical signals like current, impedance, potential, or conductance that can be measured and analyzed.¹⁸² The integration of aptamers into electrochemical biosensors has significantly advanced aptasensors, enhancing their sensitivity, specificity, and versatility for detecting a wide range of analytes. Electrochemical aptasensors employ various techniques, including potentiometric, amperometric, conductometric, impedance, and voltammetric methods. In past, researchers commonly used techniques like electrochemical impedance

spectroscopy (EIS) and voltammetry methods such as differential pulse voltammetry (DPV), cyclic voltammetry (CV), and square wave voltammetry (SWV), with cyclic voltammetry (CV) being particularly favored for analyzing redox processes and understanding electrochemical behavior. Recent advances have focused on improving sensor design for efficient antibiotic detection, utilizing signal-enhancing materials like quantum dots, metal ions, methylene blue, ferrocene, and ruthenium complexes.¹⁸³ Additionally, the integration of nanomaterials such as AuNPs, carbon-based materials (*e.g.*, graphene oxide, carbon nanotubes, carbon nanofibers), metal oxides (*e.g.*, ZnO, TiO₂, NiO), and metal–organic frameworks (MOFs) significantly enhances sensor performance by improving sensitivity, conductivity, and aptamer immobilization, thus enabling rapid and low-level detection of antibiotics in complex samples.^{184–187} The sensor developed by Zhang *et al.* utilizes a Pb²⁺-dependent DNzyme in conjunction with advanced nanomaterials like AuPt@h-CeO₂ and polyethyleneimine (PEI)-functionalized molybdenum disulfide (MoS₂), leading to enhanced sensitivity in detecting ENR with detection achieving a LOD $3.08 \times 10^{-10} \mu\text{M}$.¹⁵³ Similarly, Niu *et al.* took a different approach, developed an electrochemical aptasensor using a bimetallic NiCo₂O₄@NiO nanostructure, fabricated through solvothermal and pyrolysis methods. Electrochemical testing showed an LOD of $4.65 \times 10^{-11} \mu\text{M}$.¹⁵⁴ A label-free sensor, developed by Yu *et al.* using a 3D porous chitosan-reduced graphene oxide composite, was designed to enhance sensitivity, achieving a LOD of $1.0 \times 10^{-1} \mu\text{M}$. The sensor exhibited exceptional precision, stability, selectivity, and reproducibility, establishing it as a reliable and robust choice for accurate ENR detection.¹⁵⁵ Additionally, Guo *et al.* developed a highly sensitive electrochemical aptasensor for detecting ENR in chicken samples, utilizing magnetic capture probes (MCPs) composed of magnetic nanoparticles functionalized with ENR-specific aptamers. In the presence of ENR, the aptamers bind the target, preventing hybridization with biotinylated complementary DNA (biotin-cDNA) and thereby blocking the attachment of streptavidin–horseradish peroxidase (SA-HRP), resulting in a reduced electrochemical

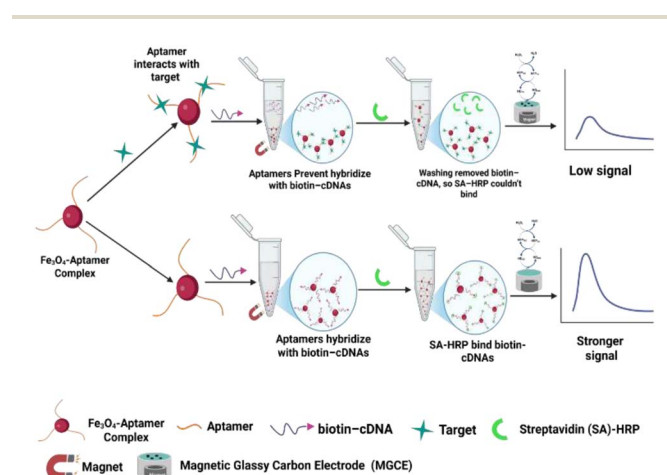


Fig. 5 Electrochemical aptasensor conceptual illustration utilizing magnetic nanoparticles for sensitive antibiotic detection.



signal. In the absence of ENR, unbound aptamers hybridize with biotin-cDNA, allowing SA-HRP to bind *via* high-affinity biotin-streptavidin interactions. After washing, MCPs are magnetically immobilized onto a magnetic glassy carbon electrode (MGCE), and detection is performed using an H₂O₂-hydroquinone-HRP catalytic system (Fig. 5), achieving a linear range of 0.01–100 ng mL⁻¹ and a detection limit of 1.5×10^{-5} μM.¹⁶⁶

For TC detection, Mohammadi *et al.* developed a sensor using electrospun carbon nanofibers and AuNPs, achieving a LOD of 1.2×10^{-4} μM and demonstrating excellent stability.³⁴ Similarly, Naseri *et al.* created an ultrasensitive sensor with a glassy carboxylated nanotubes, carbon nanofibers and carbon electrode, and achieving an impressive LOD of 2.28×10^{-12} μM.¹⁵⁶ The field has advanced with the development of highly sensitive biosensors for detecting antibiotic residues, utilizing techniques such as RecJf exonuclease-assisted target recycling (ESDR) for KAN detection.^{157,158} Additionally, magnetic mesoporous carbon materials (MMCM) on magnetic glassy carbon electrodes (MGCE) and Pd@Ti₃C₂-PEI-NCNTs composites are applied for STP detection. Both approaches provide excellent selectivity, stability, and reproducibility, making them ideal for various applications, with impressive LOD, high stability, and specificity.^{159,160} These electrochemical aptamer sensors are employed in various strategies to detect antibiotics, as summarized in Table 3. These sensors also have advantages such as wide linear ranges, low detection limits, and low costs, making them especially attractive for antibiotic detection. Compared to other methods like colorimetry and fluorescence, electrochemical aptamer films reduce non-target interference through stepwise washing. The disadvantages of electrochemical methods face challenges, including the complex procedures required for electrode surface activation, material modification, and aptamer assembly. These complexities can make large-scale sample testing difficult. Additionally, the sensitivity of aptasensors still needs improvement for practical applications, primarily due to interface effects on the electrode surface.¹²⁰

4.4. Chemiluminescence aptasensor

A chemiluminescent aptasensor is a biosensor that uses highly target specific aptamers, as recognition elements, coupled with chemiluminescence (CL) as the signal readout. This aptamer-target binding event triggers or modulates a chemiluminescent reaction, typically involving reagents like luminol and hydrogen peroxide, or enzyme-catalyzed reactions.^{176,188} The intensity of the emitted light correlates with the concentration of the target, enabling rapid, accurate, and low-level detection of a wide range of analytes (such as antibiotics, protein, toxin, or small molecule) in various sample types.¹⁸⁹ Their advantages make them promising tools for diagnostics, environmental analysis, and food safety monitoring.¹⁹⁰

In an earlier study, Hao *et al.* (2016) developed a chemiluminescent aptasensor capable of simultaneous detection of three antibiotics – OTC, TC, and KAN in milk samples. The sensor design integrated aptamers specific to each antibiotic,

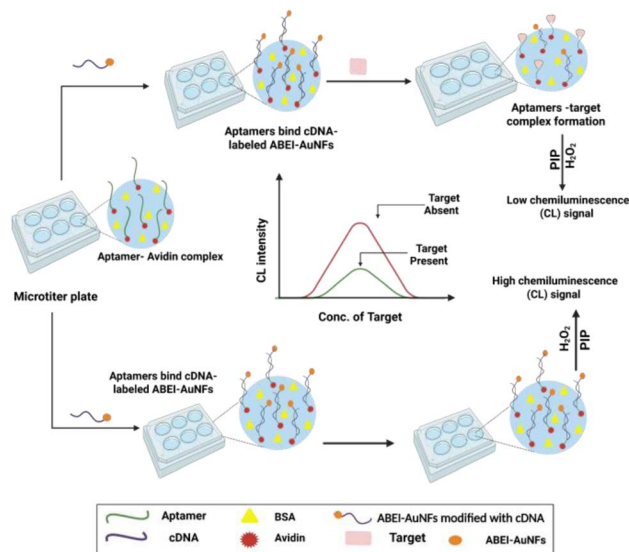


Fig. 6 Schematic representation of antibiotic detection using a chemiluminescent aptasensor based on aptamer-functionalized ABEI-AuNFs.

immobilized on a microtiter plate, with chemiluminescent signal probes constructed from ABEI (*N*-(4-aminobutyl)-*N*-ethylisoluminol)-labeled thiolated complementary DNA strands attached to flower-like gold nanostructures. Upon target binding, the aptamers underwent conformational changes, leading to displacement of the signal probes and modulation of chemiluminescence intensity (Fig. 6).

The assay demonstrated excellent sensitivity, with detection limits of 4.345×10^{-8} μM and 4.5×10^{-8} μM for OTC and TC, and 4.13×10^{-9} μM for KAN. These results underscore the sensor's potential for multiplex, low-level, and reliable detection of antibiotic residues in food safety applications.¹⁷⁶ Similarly, Leung *et al.* (2013) developed an aptamer-based switch-on luminescent probe for the sensitive and selective detection of the antibiotic kanamycin in aqueous solutions. The assay combines a luminescent platinum(II) complex and the KAN aptamer. In the absence of KAN, the luminescence of the platinum(II) complex bound to the oligonucleotide remains weak. However, upon KAN binding, the aptamer undergoes a structural transition from a random coil to a defined conformation featuring a hairpin loop, which promotes intercalation of the platinum(II) complex into the folded aptamer, thereby enhancing the luminescence signal ("switch-on" response). This conformational switch allows highly selective and sensitive detection, with a detection limit of 143 μM. The method is simple, cost-effective, and shows strong potential for applications in food safety.¹⁷³ Additionally, Lin *et al.* (2019) reported a fluorescence-based aptasensor for the rapid and sensitive detection of KAN residues using luminescent carbon nanodots functionalized with a KAN-specific aptamer. The sensing mechanism is based on fluorescence-based aptamer-linked immunosorbent assay (FALIA) that allows highly selective and sensitive detection, with a detection limit of 1.032×10^{-13}



μM .¹⁷⁴ Antibiotic detection using chemiluminescence aptasensors summarized in Table 3.

4.5. Surface plasmon resonance (SPR) aptasensor

SPR, a label-free optical detection method, emerged as real-time monitoring of various biological and chemical targets. In label-free detection, specialized tags or dyes are not required, thus allowing the sensitive measurement of target analytes. SPR detects changes in the refractive index near a metal surface when biomolecules bind to it (Fig. 7).¹⁹¹

In recent years, aptamer-based SPR sensors have gained prominence due to their specificity, simplicity, and cost-effectiveness.¹⁹² The fundamental steps involved in an aptamer based SPR sensor include the immobilization of aptamer, interaction with the target, and signal detection. When a solution containing the target molecule flows over the sensor, the aptamers immobilized on the sensor surface specifically bind to the target molecules. This binding changes the refractive index, resulting in a shift in the SPR angle, which directly correlates with the concentration of the target molecule.¹⁹³ Application of SPR-aptamer based biosensors are valued to quantification of low molecular weight compounds in different broad sectors such as food, clinical, agriculture, and environment. Écija-Arenas *et al.* developed a SPR aptamer-based biosensor designed to detect KAN residues in cow milk samples, achieving a LOD of $2.85 \times 10^{-1} \mu\text{M}$.¹⁷⁷ In their study, the aptamer was immobilized on the sensor surface using two types of graphene, *i.e.*, reduced graphene oxide (rGO) and chemical vapor deposition (CVD) graphene. The most significant result was observed in the case of CVD graphene.¹⁷⁹ In another study, Cappi and team designed a label-free, portable, palm-sized transmission-localized SPR-DNA aptamer sensing setup to precisely detect the tobramycin residues from the blood serum with a LOD of $3.4 \mu\text{M}$.¹⁷⁸ SPR aptamer sensors provide an advanced solution for antibiotic detection, combining high sensitivity, rapid

response times, label-free and real-time detection, and a simple experimental setup, making them essential tools for environmental monitoring. However, it does have some limitations, such as the potential high cost of the transducer and its focus on single-target detection. Further antibiotic detection using SPR aptasensors summarized in Table 3.

4.6. Lateral flow strip aptasensor

Lateral flow assays (LFAs) are rapid, low-cost, paper-based, point-of-care (POC) diagnostic tools used to detect specific analytes in liquid samples.¹⁹⁴ They offer high sensitivity and selectivity, making them ideal for healthcare, food safety, and environmental testing. LFAs also promote consumer self-testing adoption.¹⁹⁵ LFAs combine a chromatographic system that separates mixtures on a membrane with a biochemical reaction between antibodies and antigens or nucleic acids and target molecules.¹⁹⁶ LFAs use aptamers and nucleic acids as bio-recognition components in a strip form. They consist of three main parts: recognition, reaction, and signal transduction, integrated onto a paper strip with five components: sample pad, conjugate pad, membrane, absorbent pad, and backing plate.¹⁸⁵ A standard LFA strip has a backing plate for structural support, with overlapping components (2–3 mm) that ensure efficient liquid movement over the strip.¹⁹⁷ The sample pad, made of cellulose acetate, deposits fluid and may contain buffer salts to aid movement. The conjugate pad, made of materials like glass fiber, holds the bio-recognition element and releases it upon contact with the sample. The nitrocellulose membrane has a test line (TL) and control line (CL) for affinity assays, while the absorbent pad collects excess fluid.¹⁹⁸ In aptamer-based LFAs, the sample moves *via* capillary action to the conjugate pad, where the analyte binds to the labeled antibody. The complex then reaches the nitrocellulose membrane, where the TL captures it, and the CL ensures proper flow. The TL shows a colorimetric or fluorescent signal for detection, while the CL verifies sample flow. The absorbent pad collects excess liquid.¹⁹⁵

In sandwich aptamer-based LFAs, large molecules like pathogens are detected using two aptamers: the primary aptamer, conjugated to AuNPs, on the conjugate pad, and the biotinylated secondary aptamer on the TL. The analyte forms a complex with the primary aptamer, migrating to the TL where it's captured by the secondary aptamer. A positive result shows two red bands (TL and CL), while a negative result shows only one at the CL (Fig. 8).^{195,199}

In competitive aptamer-based LFAs, small molecules are detected by competing for aptamer binding between the sample's target molecules and those immobilized on the TL. Targets in the sample and TL compete for the aptamer, with the signal negatively correlated with the amount of target in the sample. A weak or absent signal at the TL indicates the presence of target molecules, while a stronger signal suggests their absence. The CL verifies the flow system^{35,200} (Fig. 9).

The second strategy involves target molecules competing with an immobilized complementary sequence on the TL for aptamer binding.¹⁸⁰ When an aptamer sequence undergoes structural changes, it can disrupt Watson–Crick base pairing

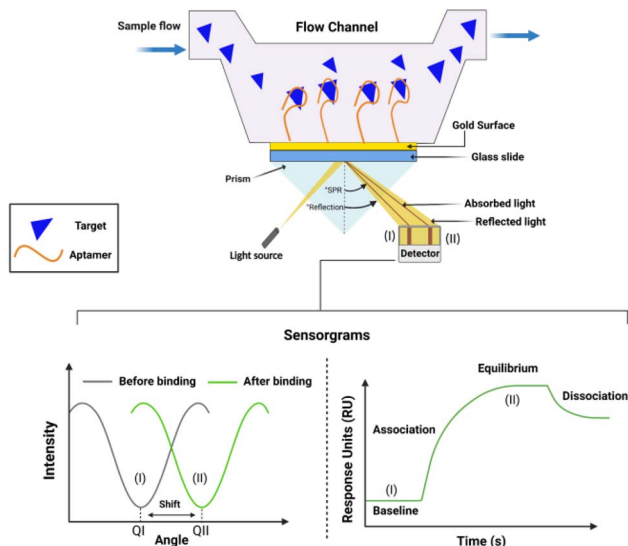


Fig. 7 Surface plasmon resonance-based aptasensor for antibiotics detection.



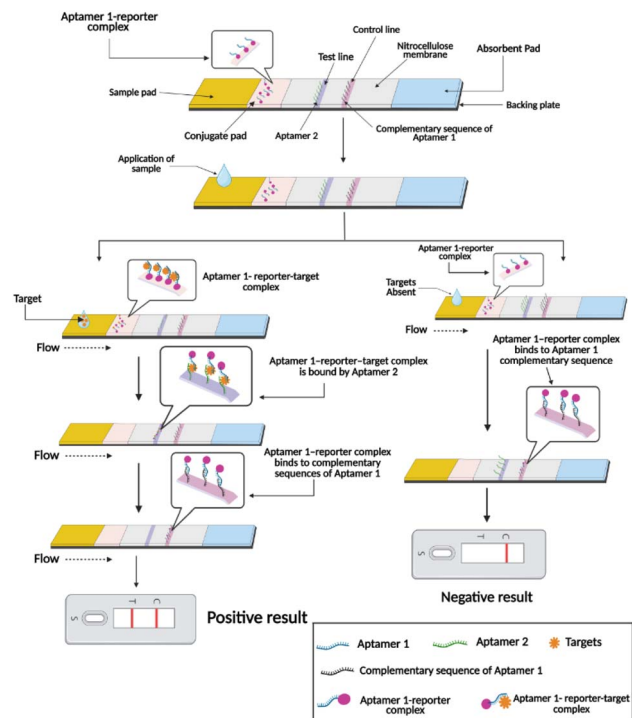


Fig. 8 Aptamer-LFAs sandwich assay: dual aptamer for targeted analyte detection.

and cause target-induced dissociation. In this strategy, an oligonucleotide partially complementary to the aptamer is attached to the TL. The target competes with this sequence,

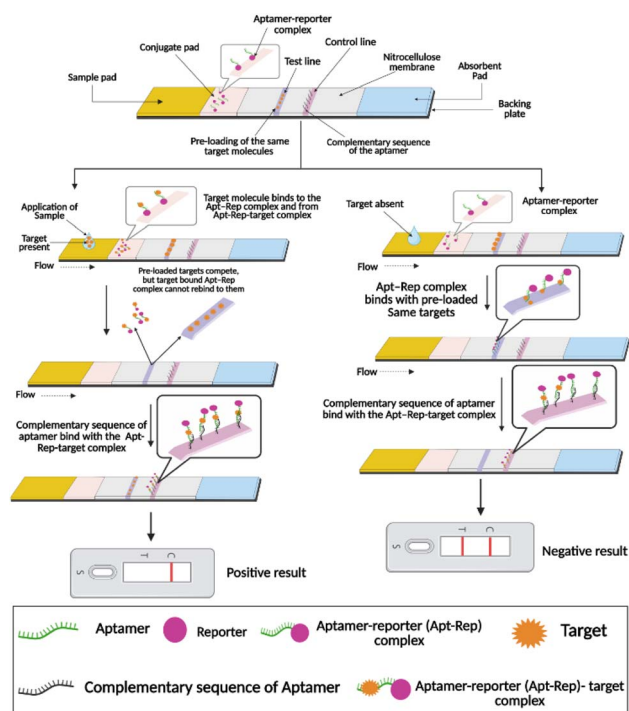


Fig. 9 Competitive aptamer-LFA: binding competition alters TL signal and validation process.

resulting in a weak or no signal on the TL. Without the target, a strong band appears as the aptamer/reporter complex is captured by the complementary sequence in Fig. 10.¹⁹⁹

Applications of aptamer-based LFAs detection antibiotics such as Ou *et al.* developed a magnetic microsphere-based aptamer-cDNA duplex LFAs to detect KAN in milk and honey. The assay worked in two steps: (1) KAN in the sample displaced cDNA from the aptamer-cDNA duplex conjugated to MMS, and (2) the released cDNA was applied to the LFAs strip, where it formed a sandwich structure with immobilized capture DNA1 and DNA2 on the TL and CL. The thresholds for visual detection in the experiment were 50 nM, whereas the quantified LOD was $4.96 \times 10^{-3} \mu\text{M}$.³⁵ Birader *et al.* developed an aptamer-based LFAs to detect OTC in milk, with the quantified LOD in OTC at $1.08 \times 10^{-4} \mu\text{M}$ within 10 minutes.¹⁸⁰ These sensors are employed in various strategies to detect antibiotics, as summarized in Table 3, which details the analytes, detection methods, and LOD. Aptamer-based LFAs offer high specificity, stability, cost-effectiveness, and flexibility, making them ideal for detecting small molecules. Their user friendliness, affordability, and portability also make them particularly well-suited for POC diagnostics. However, they have some limitations, such as limited quantitative accuracy, sample matrix interference, and the need for liquid samples. Their performance can also be affected by environmental factors like temperature and pH. Careful handling is required for reliable results, and they are typically qualitative, indicating only the presence or absence of a target analyte.

Additionally, we included a comparative analysis in Table 4 to benchmark aptasensor's performance against standard

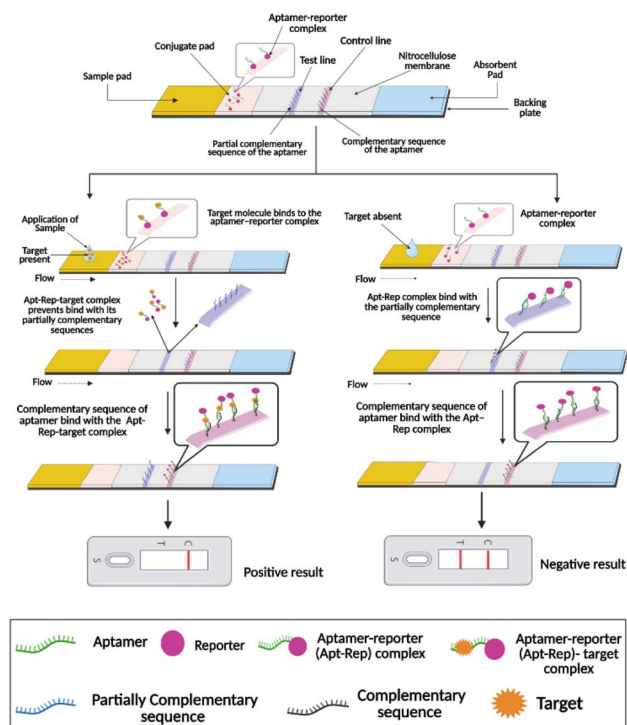


Fig. 10 Competitive aptamer-LFA: target binding controls signal by affecting partial complementary aptamer sequence on TL.



Table 4 Comparison of detection performance between standard analytical methods and aptamer-based sensors

Analytes	Technique	LOD (μM)	Matrix	Reference
KAN	Cemiluminescent aptasensor	1.032×10^{-13}	Milk	174
	Fluorescence aptasensor	5.3×10^{-5}	Milk	132
	HPLC-ELSD	1.03×10^3	Foods of animal origin	201
TC	Electrochemical aptasensor	2.28×10^{-12}	Milk	156
	Colorimetric aptasensor	4.13×10^{-12}	Milk	31
	HPLC-PDA	5.63×10^{-4}	Bovine milk	202
		2.25×10^{-1}	Milk	
	HPLC-DAD	1.23×10^1	Milk	203
OTC	Cemiluminescent aptasensor	4.345×10^{-8}	Milk	176
	HPLC-PDA	1.09×10^{-4}	Bovine milk	202
	HPLC-DAD	1.954×10^{-3}	Milk	204
	LC-MS/MS	6.52	Chicken eggs	201
	Capillary electrophoresis	1.52×10^2	Milk	205
AMP	LFAs aptasensor	1.72×10^{-8}	Milk	180
TC	Colorimetric aptasensor	2.25×10^{-7}	Honey	141
ENR	Electrochemical aptasensor	4.65×10^{-11}	—	154
	Electrochemical aptasensor	3.08×10^{-10}	Water, milk	153
	Colorimetric aptasensor	6.96×10^{-12}	Fish	115
	Fluorescence aptasensor	2.23×10^{-5}	Spiked milk	128
	LC-MS/MS	3.90×10^{-1}	Chicken eggs	201

detection methods, highlighting its relative sensitivity and practical applicability.

5 Conclusion and future prospective

Antibiotic contamination poses a serious threat to both public health and the environment, largely driven by the excessive use and improper disposal of antibiotics in the medical, agricultural, and aquaculture sectors. While conventional detection techniques such as HPLC, GC-MS, and LC-MS/MS offer high accuracy and reliability, they are often hindered by high operational costs, time-consuming procedures, and the requirement for skilled personnel and complex instrumentation. To address these limitations, aptamer-based biosensors have emerged as a powerful alternative, offering high specificity and sensitivity, rapid on-site detection, cost-effectiveness, and ease of miniaturization. This review has highlighted substantial advancements in aptasensor technologies, encompassing platforms such as colorimetric, fluorescent, electrochemical, chemiluminescent, SPR, and lateral flow assays. These methods have shown great promise in detecting antibiotic residues across a range of samples including food, water, and biological fluids, supporting applications in food safety, environmental monitoring, and clinical diagnostics. Nevertheless, the translation of aptamer biosensors into fully operational, field-deployable tools remains an evolving challenge. The integration of these sensors with microfluidic devices and wireless communication technologies could further enhance real-time detection capabilities and data accessibility. To fully unlock their potential, ongoing research must prioritize improving aptamer stability,

enhancing device robustness and multiplexing capabilities, and ensuring compliance with regulatory standards to support widespread adoption in point-of-care and environmental surveillance applications. Future development should focus on creating portable, user-friendly diagnostic systems—such as handheld readers, paper-based lateral flow devices, and smartphone-integrated platforms—to facilitate routine monitoring, especially in resource-limited or decentralized settings.

Data availability

No primary research results, software or code have been included and no new data were generated or analysed as part of this review.

Author contributions

DD, JC, PM, RM and AKM: writing – original draft. AKM: conceptualization. JC, RM and AKM – review & editing.

Conflicts of interest

There are no conflicts to declare.

Acknowledgements

D. D. would like to acknowledge the Council of Scientific and Industrial Research, Government of India, for the CSIR-JRF fellowship (CSIR-JRF; File No. 09/1224(18914)/2024-EMR-I). P. M. would like to acknowledge Swami Vivekananda Merit-cum-Means scholarship (Application ID: WBP241720165040).



R. M. would to acknowledge the DST, Govt. of India, for the DST-INSPIRE Fellowship (DST-INSPIRE-SRF; INSPIRE CODE-IF190457) and A. K. M. would like to acknowledge DST-SERB India (EEQ/2021/000058) for financial support.

Notes and references

- M. L. Barreto, M. G. Teixeira and E. H. Carmo, *J. Epidemiol. Community Health*, 2006, **60**, 192–195.
- E. Tognotti, *Emerg. Infect. Dis.*, 2013, **19**, 254–259.
- H. H. Farooqui, S. Selvaraj, A. Mehta and D. L. Heymann, *PLoS One*, 2018, **13**, e0204805.
- J. I. R. Castanon, *Poult. Sci.*, 2007, **86**, 2466–2471.
- M. Wang and J. C. Tang, *J. Agro-Environ. Sci.*, 2010, **29**, 261–266.
- N. Czekalski, E. Gascón Díez and H. Bürgmann, *ISME J.*, 2014, **8**, 1381–1390.
- A. J. Browne, M. G. Chipeta, G. Haines-Woodhouse, E. P. A. Kumaran, B. H. K. Hamadani, S. Zaraq, N. J. Henry, A. Deshpande, R. C. Reiner, N. P. J. Day, A. D. Lopez, S. Dunachie, C. E. Moore, A. Stergachis, S. I. Hay and C. Dolecek, *Lancet Planet. Health*, 2021, **5**, e893–e904.
- European Centre for Disease Prevention and Control, *Antimicrobial Resistance Surveillance in Europe: Annual Report of the European Antimicrobial Resistance Surveillance Network (EARS Net) 2015*, Publications Office, LU, 2017.
- L. Serwecińska, *Water*, 2020, **12**, 3313.
- Y. Luan, N. Wang, C. Li, X. Guo and A. Lu, *Antibiotics*, 2020, **9**, 787.
- J. O'Neill, *Tackling Drug-Resistant Infections Globally: Final Report and Recommendations*, 2016, vol. 84.
- X. Zhang, J. Wang, Q. Wu, L. Li, Y. Wang and H. Yang, *Molecules*, 2019, **24**, 1902.
- Y. Yu, Y. Liu, W. Wang, Y. Jia, G. Zhao, X. Zhang, H. Chen and Y. Zhou, *Anal. Methods*, 2019, **11**, 5064–5069.
- Y.-J. Yu, H.-L. Wu, H.-Y. Fu, J. Zhao, Y.-N. Li, S.-F. Li, C. Kang and R.-Q. Yu, *J. Chromatogr. A*, 2013, **1302**, 72–80.
- T. Van Den Meersche, E. V. Pamel, C. V. Poucke, L. Herman, M. Heyndrickx, G. Rasschaert and E. Daeseleire, *J. Chromatogr. A*, 2016, **1429**, 248–257.
- S. Yang, X. Zhu, J. Wang, X. Jin, Y. Liu, F. Qian, S. Zhang and J. Chen, *Bioresour. Technol.*, 2015, **193**, 156–163.
- J. B. Arsand, L. Jank, M. T. Martins, R. B. Hoff, F. Barreto, T. M. Pizzolato and C. Sirtori, *Talanta*, 2016, **154**, 38–45.
- J. Qiu, Q. Liu, M. Zhang, X. Li, J. Zhang, R. Xiong and L. He, *Anal. Lett.*, 2020, **53**, 2235–2251.
- U. Acaroz, S. Ince, D. Arslan-Acaroz, I. Kucukkurt and A. Eryavuz, *Kafkas Univ. Vet. Fak. Derg.*, 2020, **26**, 97–102.
- M. Gbylik-Sikorska, A. Posnyiak, T. Sniegocki and J. Zmudzki, *Chemosphere*, 2015, **119**, 8–15.
- D. Moreno-González, F. J. Lara, N. Jurgovská, L. Gámiz-Gracia and A. M. García-Campaña, *Anal. Chim. Acta*, 2015, **891**, 321–328.
- G. Zhu, C. Bao, W. Liu, X. Yan, L. Liu, J. Xiao and C. Chen, *Curr. Pharm. Anal.*, 2018, **15**, 9–16.
- L. Fu, S. Mao, F. Chen, S. Zhao, W. Su, G. Lai, A. Yu and C.-T. Lin, *Chemosphere*, 2022, **297**, 134127.
- Q. U. A. Zahra, Z. Luo, R. Ali, M. I. Khan, F. Li and B. Qiu, *Nanomaterials*, 2021, **11**, 840.
- L. V. De Faria, T. P. Lisboa, N. D. S. Campos, G. F. Alves, M. A. C. Matos, R. C. Matos and R. A. A. Munoz, *Anal. Chim. Acta*, 2021, **1173**, 338569.
- Y. Zhou, C. Mahapatra, H. Chen, X. Peng, S. Ramakrishna and H. S. Nanda, *Curr. Opin. Biomed. Eng.*, 2020, **13**, 16–24.
- S. Afrasiabi, M. Pourhajibagher, R. Raoofian, M. Tabarzad and A. Bahador, *J. Biomed. Sci.*, 2020, **27**, 6.
- G. Liang, Y. Man, A. Li, X. Jin, X. Liu and L. Pan, *Microchem. J.*, 2017, **131**, 145–153.
- G. Liang, Y. Man, A. Li, X. Jin, L. Pan and X. Liu, *Microchim. Acta*, 2017, **185**, 54.
- G. Liang, Y. Man, X. Jin, L. Pan and X. Liu, *Anal. Chim. Acta*, 2016, **936**, 222–228.
- M. Liu, Z. Yang, B. Li and J. Du, *Food Chem.*, 2021, **339**, 128059.
- C. Zhou, H. Zou, C. Sun, D. Ren, W. Xiong and Y. Li, *Anal. Bioanal. Chem.*, 2018, **410**, 2981–2989.
- C.-C. Li, W.-C. Kong, J.-L. Cui, X.-L. Li, Y.-L. Meng, X.-J. Jia, X.-L. Zhang and Y.-F. Kang, *Research Square*, 2024, preprint, DOI: [10.21203/rs.3.rs-4911437/v1](https://doi.org/10.21203/rs.3.rs-4911437/v1).
- S. Mohammadi, K. P. Bagheri, R. M. Nadushan and M. Adabi, *Appl. Phys. A*, 2023, **129**, 176.
- Y. Ou, X. Jin, J. Liu, Y. Tian and N. Zhou, *Anal. Biochem.*, 2019, **587**, 113432.
- P. Kovalakova, L. Cizmas, T. J. McDonald, B. Marsalek, M. Feng and V. K. Sharma, *Chemosphere*, 2020, **251**, 126351.
- M. K. Chattopadhyay, *Front. Microbiol.*, 2014, **5**, 334.
- R. Mithuna, R. Tharanyalakshmi, I. Jain, S. Singhal, D. Sikarwar, S. Das, J. Ranjitha, D. Ghosh, M. M. Rahman and B. Das, *Emerg. Contam.*, 2024, **10**, 100389.
- F. C. Cabello, *Environ. Microbiol.*, 2006, **8**, 1137–1144.
- M. Pepi and S. Focardi, *Int. J. Environ. Res. Publ. Health*, 2021, **18**, 5723.
- J. Williams-Nguyen, J. B. Sallach, S. Bartelt-Hunt, A. B. Boxall, L. M. Durso, J. E. McLain, R. S. Singer, D. D. Snow and J. L. Zilles, *J. Environ. Qual.*, 2016, **45**, 394–406.
- L. M. Durso and K. L. Cook, *Curr. Opin. Microbiol.*, 2014, **19**, 37–44.
- D. B. Worthen, *J. Hist. Med. Allied Sci.*, 2007, **63**, 273–274.
- D. C. Rocha, C. Da Silva Rocha, D. S. Tavares, S. L. De Moraes Calado and M. P. Gomes, *Sci. Total Environ.*, 2021, **767**, 144902.
- D. Schuster, K. Axtmann, N. Holstein, C. Felder, A. Voigt, H. Färber, P. Ciorba, C. Szekat, A. Schallenberg, M. Böckmann, C. Zarfl, C. Neidhöfer, K. Smalla, M. Exner and G. Bierbaum, *Environ. Microbiol.*, 2022, **24**, 5721–5733.
- A. N. Ngigi, M. M. Magu and B. M. Muendo, *Environ. Monit. Assess.*, 2020, **192**, 18.
- N. Hanna, P. Sun, Q. Sun, X. Li, X. Yang, X. Ji, H. Zou, J. Ottoson, L. E. Nilsson, B. Berglund, O. J. Dyar, A. J. Tamhankar and C. S. Lundborg, *Environ. Int.*, 2018, **114**, 131–142.



- 48 R. Gothwal and T. Shashidhar, *Clean: Soil, Air, Water*, 2014, **43**, 479–489.
- 49 E. L. Thiang, C. W. Lee, H. Takada, K. Seki, A. Takei, S. Suzuki, A. Wang and C. W. Bong, *Ecosys. Health Sustain.*, 2021, **7**, 1926337.
- 50 M. W. Joseph, W. N. Moturi and G. M. Ogendi, *Curr. World Environ.*, 2024, **19**, 778–789.
- 51 D. G. J. Larsson and C.-F. Flach, *Nat. Rev. Microbiol.*, 2022, **20**, 257–269.
- 52 M. Amarasiri, D. Sano and S. Suzuki, *Crit. Rev. Environ. Sci. Technol.*, 2020, **50**, 2016–2059.
- 53 National Research Council (US) Committee to Study the Human Health Effects of Subtherapeutic Antibiotic Use in Animal Feeds, *The Effects on Human Health of Subtherapeutic Use of Antimicrobials in Animal Feeds*, National Academies Press, Washington (DC), 1980.
- 54 L. Zhao, Y. H. Dong and H. Wang, *Sci. Total Environ.*, 2010, **408**, 1069–1075.
- 55 A. Göbel, C. S. McArdell, M. J.-F. Suter and W. Giger, *Anal. Chem.*, 2004, **76**, 4756–4764.
- 56 N. Kemper, *Ecol. Indic.*, 2008, **8**, 1–13.
- 57 J.-F. Yang, G.-G. Ying, J.-L. Zhao, R. Tao, H.-C. Su and F. Chen, *Sci. Total Environ.*, 2010, **408**, 3424–3432.
- 58 K. Kümmerer, *Chemosphere*, 2009, **75**, 417–434.
- 59 D. G. J. Larsson, C. De Pedro and N. Paxeus, *J. Hazard. Mater.*, 2007, **148**, 751–755.
- 60 S. Jechalke, H. Heuer, J. Siemens, W. Amelung and K. Smalla, *Trends Microbiol.*, 2014, **22**, 536–545.
- 61 X. Wang, D. Ryu, R. H. Houtkooper and J. Auwerx, *BioEssays*, 2015, **37**, 1045–1053.
- 62 V. Minden, A. Deloy, A. M. Volkert, S. D. Leonhardt and G. Pufal, *AoB Plants*, 2017, **9**, plx010.
- 63 W. S. Darwish, Y. Ikenaka and M. Ishizuka, *Jpn. J. Vet. Res.*, 2013, **61**, S48–S53.
- 64 D. V. Patangia, C. Anthony Ryan, E. Dempsey, R. Paul Ross and C. Stanton, *Microbiologyopen*, 2022, **11**, e1260.
- 65 C. J. Damman, S. I. Miller, C. M. Surawicz and T. L. Zisman, *Am. J. Gastroenterol.*, 2012, **107**, 1452–1459.
- 66 L. M. Cox, S. Yamanishi, J. Sohn, A. V. Alekseyenko, J. M. Leung, I. Cho, S. G. Kim, H. Li, Z. Gao, D. Mahana, J. G. Zárate Rodríguez, A. B. Rogers, N. Robine, P. Loke and M. J. Blaser, *Cell*, 2014, **158**, 705–721.
- 67 I. Cho, S. Yamanishi, L. Cox, B. A. Methé, J. Zavadil, K. Li, Z. Gao, D. Mahana, K. Raju, I. Teitler, H. Li, A. V. Alekseyenko and M. J. Blaser, *Nature*, 2012, **488**, 621–626.
- 68 D. L. Robertson and G. F. Joyce, *Nature*, 1990, **344**, 467–468.
- 69 C. Tuerk and L. Gold, *Science*, 1990, **249**, 505–510.
- 70 A. D. Ellington and J. W. Szostak, *Nature*, 1990, **346**, 818–822.
- 71 A. D. Ellington and J. W. Szostak, *Nature*, 1992, **355**, 850–852.
- 72 A. S. Shraim, B. A. Abdel Majeed, M. A. Al-Binni and A. Hunaiti, *ACS Pharmacol. Transl. Sci.*, 2022, **5**, 1211–1227.
- 73 J. Zhou and J. Rossi, *Nat. Rev. Drug Discov.*, 2017, **16**, 181–202.
- 74 C. Lyu, I. M. Khan and Z. Wang, *Talanta*, 2021, **229**, 122274.
- 75 D.-M. Kim, M.-J. Go, J. Lee, D. Na and S.-M. Yoo, *Molecules*, 2021, **26**, 5187.
- 76 T. Hianik, *Biosensors*, 2021, **11**, 177.
- 77 G. Mayer, *Angew. Chem., Int. Ed.*, 2009, **48**, 2672–2689.
- 78 C. Kratschmer and M. Levy, *Nucleic Acid Ther.*, 2017, **27**, 335–344.
- 79 D. V. Morrissey, K. Blanchard, L. Shaw, K. Jensen, J. A. Lockridge, B. Dickinson, J. A. McSwiggen, C. Vargeese, K. Bowman, C. S. Shaffer, B. A. Polisky and S. Zinnen, *Hepatology*, 2005, **41**, 1349–1356.
- 80 F. Bottari, E. Daems, A.-M. De Vries, P. Van Wielendaele, S. Trashin, R. Blust, F. Sobott, A. Maddar, J. C. Martins and K. De Wael, *J. Am. Chem. Soc.*, 2020, **142**, 19622–19630.
- 81 X. Tao, F. He, X. Liu, F. Zhang, X. Wang, Y. Peng and J. Liu, *Microchim. Acta*, 2020, **187**, 668.
- 82 Y. Zhao, A. Z. Li and J. Liu, *Environ. Health*, 2023, **1**, 102–109.
- 83 Y. Yang, S. Yin, Y. Li, D. Lu, J. Zhang and C. Sun, *TrAC, Trends Anal. Chem.*, 2017, **95**, 1–22.
- 84 S. Li and W. S. Choe, *J. Biotechnol.*, 2008, **136**, S86.
- 85 H. X. Liu, C. Z. Wang, B. X. Zhang and K. D. Xu, *Chin. J. Anal. Chem.*, 2017, 1971–1979.
- 86 F. Li, Z. Yu, X. Han and R. Y. Lai, *Anal. Chim. Acta*, 2019, **1051**, 1–23.
- 87 E. B. Bahadır and M. K. Sezgentürk, *TrAC, Trends Anal. Chem.*, 2016, **76**, 1–14.
- 88 M. Zuker, *Nucleic Acids Res.*, 2003, **31**, 3406–3415.
- 89 A.-Y. Lee, N.-R. Ha, I.-P. Jung, S.-H. Kim, A.-R. Kim and M.-Y. Yoon, *Anal. Biochem.*, 2017, **531**, 1–7.
- 90 Y. Zhao, B. Gao, Y. Chen and J. Liu, *Analyst*, 2023, **148**, 1507–1513.
- 91 X. Han, Y. Zhang, J. Nie, S. Zhao, Y. Tian and N. Zhou, *Microchim. Acta*, 2017, **185**, 4.
- 92 Y. Ding, Z. Gao and H. Li, *Sens. Actuators, B*, 2021, **343**, 130113.
- 93 D. H. Burke, D. C. Hoffman, A. Brown, M. Hansen, A. Pardi and L. Gold, *Chem. Biol.*, 1997, **4**, 833–843.
- 94 Y. Zhu, P. Chandra, K.-M. Song, C. Ban and Y.-B. Shim, *Biosens. Bioelectron.*, 2012, **36**, 29–34.
- 95 M. G. Wallis, U. von Ahsen, R. Schroeder and M. Famulok, *Chem. Biol.*, 1995, **2**, 543–552.
- 96 G. Liang, L. Song, Y. Gao, K. Wu, R. Guo, R. Chen, J. Zhen and L. Pan, *Toxics*, 2023, **11**, 513.
- 97 S. R. Han, J. Yu and S.-W. Lee, *Biochem. Biophys. Res. Commun.*, 2014, **448**, 397–402.
- 98 J. H. Niazi, S. J. Lee, Y. S. Kim and M. B. Gu, *Bioorg. Med. Chem.*, 2008, **16**, 1254–1261.
- 99 R. Chinnappan, S. Eissa, A. Alotaibi, A. Siddiqua, O. A. Alsager and M. Zourob, *Anal. Chim. Acta*, 2020, **1101**, 149–156.
- 100 M. Majdinasab, K. Mitsubayashi and J. L. Marty, *Trends Biotechnol.*, 2019, **37**, 898–915.
- 101 T. Yang, Z. Luo, Y. Tian, C. Qian and Y. Duan, *TrAC, Trends Anal. Chem.*, 2020, **124**, 115795.
- 102 D. Zhu, B. Liu and G. Wei, *Biosensors*, 2021, **11**, 259.



- 103 G. Ghodake, S. Shinde, R. G. Saratale, A. Kadam, G. D. Saratale, A. Syed, N. Marraiki, A. M. Elgorban and D. Kim, *J. Sci. Food Agric.*, 2020, **100**, 874–884.
- 104 M. Majdinasab, R. K. Mishra, X. Tang and J. L. Marty, *TrAC, Trends Anal. Chem.*, 2020, **127**, 115883.
- 105 H. Katano, Y. Kuroda, S. Taira, C. Maruyama and Y. Hamano, *Anal. Sci.*, 2017, **33**, 499–503.
- 106 N. Sethu, S. Krishnakumar, V. Mitra, C. Tagad and R. Vyas, *Sens. Acutators Rep.*, 2023, **5**, 100151.
- 107 L. Zhang, Y. Mazouzi, M. Salmain, B. Liedberg and S. Boujday, *Biosens. Bioelectron.*, 2020, **165**, 112370.
- 108 J. Simon, S. Udayan, E. S. Bindiya, S. G. Bhat, V. P. N. Nampoori and M. Kailasnath, *Anal. Biochem.*, 2021, **612**, 113975.
- 109 W. Bai, C. Zhu, J. Liu, M. Yan, S. Yang and A. Chen, *Environ. Toxicol. Chem.*, 2015, **34**, 2244–2249.
- 110 N. Fahimi-Kashani and M. R. Hormozi-Nezhad, *Anal. Chem.*, 2016, **88**, 8099–8106.
- 111 K.-M. Song, M. Cho, H. Jo, K. Min, S. H. Jeon, T. Kim, M. S. Han, J. K. Ku and C. Ban, *Anal. Biochem.*, 2011, **415**, 175–181.
- 112 Y. Xu, T. Han, X. Li, L. Sun, Y. Zhang and Y. Zhang, *Anal. Chim. Acta*, 2015, **891**, 298–303.
- 113 N.-R. Ha, I.-P. Jung, S.-H. Kim, A.-R. Kim and M.-Y. Yoon, *Process Biochem.*, 2017, **62**, 161–168.
- 114 T. Zhao, Q. Chen, Y. Wen, X. Bian, Q. Tao, G. Liu and J. Yan, *Food Chem.*, 2022, **377**, 132072.
- 115 Y. Du, Y. Zhou, Y. Wen, X. Bian, Y. Xie, W. Zhang, G. Liu and J. Yan, *Microchim. Acta*, 2019, **186**, 840.
- 116 Z. Zhang, Y. Tian, P. Huang and F.-Y. Wu, *Talanta*, 2020, **208**, 120342.
- 117 S. Wang, S. Gao, S. Sun, Y. Yang, Y. Zhang, J. Liu, Y. Dong, H. Su and T. Tan, *RSC Adv.*, 2016, **6**, 45645–45651.
- 118 R. Wang, Q. Zhang, Y. Zhang, H. Shi, K. T. Nguyen and X. Zhou, *Anal. Chem.*, 2019, **91**, 15811–15817.
- 119 B. Lin, Y. Yu, Y. Cao, M. Guo, D. Zhu, J. Dai and M. Zheng, *Biosens. Bioelectron.*, 2018, **100**, 482–489.
- 120 B. Sequeira-Antunes and H. A. Ferreira, *Biomedicines*, 2023, **11**, 3201.
- 121 G. Zheng, L. Zhao, D. Yuan, J. Li, G. Yang, D. Song, H. Miao, L. Shu, X. Mo, X. Xu, L. Li, X. Song and Y. Zhao, *Biosens. Bioelectron.*, 2022, **198**, 113827.
- 122 S. Ng, H. S. Lim, Q. Ma and Z. Gao, *Theranostics*, 2016, **6**, 1683–1702.
- 123 B. J. Alyamani, O. A. Alsager and M. Zourob, *Sensors*, 2019, **19**, 4181.
- 124 S. H. Jalalian, S. M. Taghdisi, N. M. Danesh, H. Bakhtiari, P. Lavaee, M. Ramezani and K. Abnous, *Anal. Methods*, 2015, **7**, 2523–2528.
- 125 S. Yang, C. Li, H. Zhan, R. Liu, W. Chen, X. Wang and K. Xu, *J. Nanobiotechnol.*, 2023, **21**, 22.
- 126 A. Bahreyni, H. Luo, M. Ramezani, M. Alibolandi, V. Soheili, N. M. Danesh, M. S. Ashjaei, K. Abnous and S. M. Taghdisi, *Spectrochim. Acta, Part A*, 2021, **246**, 119009.
- 127 S. M. Taghdisi, N. M. Danesh, M. A. Nameghi, M. Ramezani and K. Abnous, *Food Chem.*, 2016, **203**, 145–149.
- 128 Z. Shang, P. Ma, I. M. Khan, Y. Zhang and Z. Wang, *Food Control*, 2023, **145**, 109437.
- 129 S. Dolati, M. Ramezani, M. S. Nabavinia, V. Soheili, K. Abnous and S. M. Taghdisi, *Anal. Biochem.*, 2018, **549**, 124–129.
- 130 W.-C. Kong, C.-C. Li, X.-L. Zhang, J.-L. Cui, X.-L. Li, X.-J. Jia, Y.-L. Meng and Y.-F. Kang, *Anal. Lett.*, 2024, 1–13.
- 131 J. Wang, T. Lu, Y. Hu, X. Wang and Y. Wu, *Spectrochim. Acta, Part A*, 2020, **226**, 117651.
- 132 L. Xie, C. Fan, Y. Liu, Q. Chen and X. Chen, *Anal. Chim. Acta*, 2024, **1308**, 342659.
- 133 D. Xu, L. Shan, B. Guo, J. Wang, Q. Huang, S. Wang, F. Li, S. Wu, W. Wang and J. Chen, *Food Chem.*, 2025, **478**, 143291.
- 134 Z. Liu, W. Yang, H. Lin, M. Zhang and C. Sun, *Biosensors*, 2025, **15**, 252.
- 135 J. Zhao, Y. Wu, H. Tao, H. Chen, W. Yang and S. Qiu, *RSC Adv.*, 2017, **7**, 38471–38478.
- 136 X. Zhou, L. Wang, G. Shen, D. Zhang, J. Xie, A. Mamut, W. Huang and S. Zhou, *Microchim. Acta*, 2018, **185**, 355.
- 137 Y. Luo, J. Xu, Y. Li, H. Gao, J. Guo, F. Shen and C. Sun, *Food Control*, 2015, **54**, 7–15.
- 138 Q. Ma, Y. Wang, J. Jia and Y. Xiang, *Food Chem.*, 2018, **249**, 98–103.
- 139 Y. S. Kwon, N. H. A. Raston and M. B. Gu, *Chem. Commun.*, 2014, **50**, 40–42.
- 140 A. Wang, H. Zhao, X. Chen, B. Tan, Y. Zhang and X. Quan, *Anal. Biochem.*, 2017, **525**, 92–99.
- 141 Y. Tang, J. Zhang, J.-H. Liu, I. Gapparov, S. Wang, Y. Dong, H. Su and T. Tan, *Anal. Methods*, 2017, **9**, 1133–1140.
- 142 J. Zhou, Y. Li, W. Wang, Z. Lu, H. Han and J. Liu, *Langmuir*, 2020, **36**, 11490–11498.
- 143 P. Lavaee, N. M. Danesh, M. Ramezani, K. Abnous and S. M. Taghdisi, *Microchim. Acta*, 2017, **184**, 2039–2045.
- 144 Y. Sun, T. Qi, Y. Jin, L. Liang and J. Zhao, *RSC Adv.*, 2021, **11**, 10054–10060.
- 145 Y. Tian, Y. Mou, W. Zhang, Z. Sun, Y. Yin, L. Han, D. Chen, Y. Guo, X. Sun, F. Li and Y. Wu, *Biosens. Bioelectron.*, 2025, **268**, 116911.
- 146 M. Li, R. Huang, X. Liao, Z. Zhou, L. Zou and B. Liu, *Anal. Methods*, 2023, **15**, 843–848.
- 147 Z. Luo, Y. Wang, X. Lu, J. Chen, F. Wei, Z. Huang, C. Zhou and Y. Duan, *Anal. Chim. Acta*, 2017, **984**, 177–184.
- 148 B. Tan, H. Zhao, L. Du, X. Gan and X. Quan, *Biosens. Bioelectron.*, 2016, **83**, 267–273.
- 149 Y. Wang, N. Gan, Y. Zhou, T. Li, Y. Cao and Y. Chen, *Biosens. Bioelectron.*, 2017, **87**, 508–513.
- 150 Y. Duan, L. Wang, Z. Gao, H. Wang, H. Zhang and H. Li, *Talanta*, 2017, **165**, 671–676.
- 151 K. Ling, H. Jiang, L. Zhang, Y. Li, L. Yang, C. Qiu and F.-R. Li, *Anal. Bioanal. Chem.*, 2016, **408**, 3593–3600.
- 152 M. D. Simmons, L. M. Miller, M. O. Sundström and S. Johnson, *Antibiotics*, 2020, **9**, 655.
- 153 B. Zhang, L. Lv, X. Ma, L. Xie, M. Lin, H. Chen and B. He, *Biosens. Bioelectron.*, 2022, **210**, 114296.
- 154 Z. Niu, S. Wang, R. Luo, P. Wei, K. Li, W. Wang and Q. Yang, *Anal. Methods*, 2023, **15**, 1441–1451.



- 155 Q. Yu, H. Yang and Y. Yang, *J. Food Meas. Char.*, 2023, **18**, 87–94.
- 156 M. Naseri, A. Niazi, K. Bagherzadeh, E. Konozi and H. R. Samadikhah, *Food Chem.*, 2023, **421**, 136195.
- 157 Q. Xiao, D. Zhang, M. Yang, S. Liu, Y. Fang and S. Huang, *J. Anal. Test.*, 2024, **9**, 96–108.
- 158 Y. Jin, Y. Zhang, H. Xu, X. Lu, Y. Yuan and W. Zhang, *Food Control*, 2024, **161**, 110390.
- 159 L. Wang, H. Wang, S. Huang, F. Wu and X. Niu, *Food Chem.*, 2023, **403**, 134399.
- 160 Y. Hui, D. Yang, L. Wei, M. Pu, Y. Mao, X. Chen and B. Wang, *Food Chem.*, 2024, **432**, 137271.
- 161 Y. Zhou, F. Li, H. Wu, Y. Chen, H. Yin, S. Ai and J. Wang, *Sens. Actuators, B*, 2019, **296**, 126664.
- 162 Q. Zhang, F. Li, X. Li, Y. Liu and J. Han, *Int. J. Electrochem. Sci.*, 2021, **16**, 211143.
- 163 F. Hong, X. Chen, Y. Cao, Y. Dong, D. Wu, F. Hu and N. Gan, *Biosens. Bioelectron.*, 2018, **112**, 202–208.
- 164 X. Yao, J. Shen, Q. Liu, H. Fa, M. Yang and C. Hou, *Anal. Methods*, 2020, **12**, 4967–4976.
- 165 H. Peng, Y. Hui, L. Zhang, F. Zhang, Y. Liu, J. Zheng, R. Jia, Y. Song and B. Wang, *Sens. Actuators, B*, 2022, **368**, 132119.
- 166 X. Guo, F. Li, X. Zhu, P. Zhang, Y. Liu and Z. Li, *Int. J. Electrochem. Sci.*, 2024, **19**, 100537.
- 167 B. Xie, H. Peng, R. Zhang, C. Wang and Y. He, *J. Phys. Chem. C*, 2021, **125**, 5678–5683.
- 168 D. Zheng, X. Zhu, X. Zhu, B. Bo, Y. Yin and G. Li, *Analyst*, 2013, **138**, 1886.
- 169 Z. Yu and R. Y. Lai, *Talanta*, 2018, **176**, 619–624.
- 170 P. Chandra, H.-B. Noh, M.-S. Won and Y.-B. Shim, *Biosens. Bioelectron.*, 2011, **26**, 4442–4449.
- 171 A. A. Rowe, E. A. Miller and K. W. Plaxco, *Anal. Chem.*, 2010, **82**, 7090–7095.
- 172 E. González-Fernández, N. de-los-Santos-Álvarez, M. J. Lobo-Castañón, A. J. Miranda-Ordieres and P. Tuñón-Blanco, *Biosens. Bioelectron.*, 2011, **26**, 2354–2360.
- 173 K.-H. Leung, H.-Z. He, D. S.-H. Chan, W.-C. Fu, C.-H. Leung and D.-L. Ma, *Sens. Actuators, B*, 2013, **177**, 487–492.
- 174 X. Lin, J. Su, H. Lin, X. Sun, B. Liu, R. K. Kankala and S.-F. Zhou, *Talanta*, 2019, **202**, 452–459.
- 175 M. Zhao, Y. Zhuo, Y.-Q. Chai and R. Yuan, *Biomaterials*, 2015, **52**, 476–483.
- 176 L. Hao, H. Gu, N. Duan, S. Wu and Z. Wang, *Anal. Methods*, 2016, **8**, 7929–7936.
- 177 Á. Écija-Arenas, E.-M. Kirchner, T. Hirsch and J. M. Fernández-Romero, *Anal. Chim. Acta*, 2021, **1169**, 338631.
- 178 G. Cappi, F. M. Spiga, Y. Moncada, A. Ferretti, M. Beyeler, M. Bianchessi, L. Decosterd, T. Buclin and C. Guiducci, *Anal. Chem.*, 2015, **87**, 5278–5285.
- 179 N. de-los-Santos-Álvarez, M. J. Lobo-Castañón, A. J. Miranda-Ordieres and P. Tuñón-Blanco, *Biosens. Bioelectron.*, 2009, **24**, 2547–2553.
- 180 K. Birader, P. Kumar, Y. Tammineni, J. A. Barla, S. Reddy and P. Suman, *Food Chem.*, 2021, **356**, 129659.
- 181 L. Kaiser, J. Weisser, M. Kohl and H.-P. Deigner, *Sci. Rep.*, 2018, **8**, 5628.
- 182 Z. Li, M. A. Mohamed, A. M. Vinu Mohan, Z. Zhu, V. Sharma, G. K. Mishra and R. K. Mishra, *Sensors*, 2019, **19**, 5435.
- 183 N. Lu, J. Chen, Z. Rao, B. Guo and Y. Xu, *Biosensors*, 2023, **13**, 850.
- 184 M. Amiri, K. Nekoueiian and R. S. Saberi, *Anal. Bioanal. Chem.*, 2021, **413**, 673–699.
- 185 F. Li, J. Zhu, Y. Liu, Z. Lil, H. Kang and R. Li, *Int. J. Electrochem. Sci.*, 2020, **15**, 7520–7530.
- 186 D. N. Da Silva and A. C. Pereira, *Electrochem*, 2023, **4**, 553–567.
- 187 Z. Chen, M. Xie, F. Zhao and S. Han, *Foods*, 2022, **11**, 1404.
- 188 S. Cheng, H. Liu, H. Zhang, G. Chu, Y. Guo and X. Sun, *Sens. Actuators, B*, 2020, **304**, 127367.
- 189 L. Yang, H. Ni, C. Li, X. Zhang, K. Wen, Y. Ke, H. Yang, W. Shi, S. Zhang, J. Shen and Z. Wang, *Sens. Actuators, B*, 2019, **281**, 801–811.
- 190 L. Hao, N. Duan, S. Wu, B. Xu and Z. Wang, *Anal. Bioanal. Chem.*, 2015, **407**, 7907–7915.
- 191 H. H. Nguyen, J. Park, S. Kang and M. Kim, *Sensors*, 2015, **15**, 10481–10510.
- 192 S. H. Lee, Y. E. Park, J. E. Lee and H. J. Lee, *Biosens. Bioelectron.*, 2020, **154**, 112065.
- 193 C.-C. Chang, *Biosensors*, 2021, **11**, 233.
- 194 K. M. Koczula and A. Gallotta, *Essays Biochem.*, 2016, **60**, 111–120.
- 195 M. Majdinasab, M. Badea and J. L. Marty, *Pharmaceuticals*, 2022, **15**, 90.
- 196 E. B. Bahadır and M. K. Sezginürk, *TrAC, Trends Anal. Chem.*, 2016, **82**, 286–306.
- 197 H. Ye, Y. Liu, L. Zhan, Y. Liu and Z. Qin, *Theranostics*, 2020, **10**, 4359–4373.
- 198 M. Sajid, A.-N. Kawde and M. Daud, *J. Saudi Chem. Soc.*, 2015, **19**, 689–705.
- 199 T. Wang, L. Chen, A. Chikkanna, S. Chen, I. Brusius, N. Sbu and R. N. Veedu, *Theranostics*, 2021, **11**, 5174–5196.
- 200 T. Kurth, S. Witt, S. Bolten, J.-J. Waniek, C. Kortmann, A. Lavrentieva, T. Scheper and J.-G. Walter, *Biosensors*, 2019, **9**, 124.
- 201 Q. Liu, J. Li, X. Song, M. Zhang, E. Li, F. Gao and L. He, *RSC Adv.*, 2017, **7**, 1251–1259.
- 202 M. N. Uddin, A. Hasnaine, Md. S. Haque, S. Das, M. Uddin, D. Chakraborty and M. Mostafa, *J. Food Prot.*, 2024, **87**, 100279.
- 203 M. Kurjogi, Y. H. I. Mohammad, S. Alghamdi, M. Abdelrahman, P. Satapute and S. Jogaiah, *PLoS One*, 2019, **14**, e0223475.
- 204 A. Kumar, A. K. Panda and N. Sharma, *J. Food Sci. Technol.*, 2022, **59**, 95–104.
- 205 S. Dawadi, R. Thapa, B. Modi, S. Bhandari, A. P. Timilsina, R. P. Yadav, B. Aryal, S. Gautam, P. Sharma, B. B. Thapa, N. Aryal, S. Aryal, B. P. Regmi and N. Parajuli, *Processes*, 2021, **9**, 1500.

